IOWA STATE UNIVERSITY
Digital Repository

2016

Analysis of trans-epithelial electrical resistance (TEER) in organ-on-chips to study the functions of human placenta

Rajeendra Lakruwan Pemathilaka
Iowa State University

Follow this and additional works at: http://lib.dr.iastate.edu/etd

 Part of the Biomedical Commons, and the Mechanical Engineering Commons

Analysis of trans-epithelial electrical resistance (TEER) in organ-on-chips to study the functions of human placenta

by

Rajeendra Lakruwan Pemathilaka

A thesis submitted to the graduate faculty

in partial fulfillment of the requirements for the degree of

MASTER OF SCIENCE

Major: Mechanical Engineering

Program of Study Committee:
Nastaran Hashemi, Major Professor
Reza Montazami
Marit Nilsen-Hamilton

Iowa State University

Ames, Iowa

2016

TABLE OF CONTENTS

ACKNOWLEDGMENTS

Firstly, I would like to thank Dr. Nastaran Hashemi, my major professor, for the freedom, guidance and support during the course of this research. I would like to thank my committee members, Dr. Reza Montazami and Dr. Marit Nilsen-Hamilton for being a part of my master's committee.

My sincere thanks go out to my friends, colleagues, the mechanical engineering department faculty and staff for their support. I want to also thank Dr. Donald Sakaguchi at Sakaguchi labs and Amanda Brockman at Hybridoma facility, without whom, this thesis would not have been possible.

Last but not least, I would like to express my sincere gratitude to my parents, Sunil Pemathilaka and Chandrani Kusumlatha, to whom this dissertation is dedicated to, for being the strength behind me and encouraging me to achieve my goals. Also, I would like to thank my brother Hasindu and sister Narmada for supporting me along my academic career.

ABSTRACT

Organ-on a-chip technology is becoming a popular method for drug testing. Microfluidic Organ-on-a-chip eliminates the need for live objects, such as animals, to do drug testing. Although the Organ-on-a-chip devices are becoming popular, creating a microfluidic device to represent human placenta is more challenging than other organs. Current drug testing methods are considered unethical and unreliable due to drug testing on animals and cost. The human placenta is a temporary organ created during pregnancy to connect fetus and its mother to allow nutrient supply, gas exchange, waste elimination, and avoid internal infections. Researchers wanted to study how the two-way traffic reacts when it's blocked by bacteria/viruses while it transfers the nutrients/ oxygen, since the lack of transportation can affect the health of the mother and the fetus. When animal organs are used for testing on the human placenta, inconsistent results have been found due to the differences among species in physiological functions of human placental barrier, including permeability, transport of supplements, patterns of blood flow, and even in metabolic activities. Our "Placenta-on-a-chip" device is designed to represent a working placenta organ using human cells in order to imitate the nutrient/waste transfer between the maternal blood and fetal blood. HUVEC cells (endothelial) and BeWo cells (trophoblast) were used to represent the placental barrier with a high concentrated collagen coated membrane. The objective is to analyze the glucose transport between the endothelial-trophoblast barrier through the membrane. In the future, researchers will have the opportunity to use the placenta-on-a-chip model for additional research in drug testing.

Trans-epithelial electrical resistance (TEER) is a useful method to study the performance of the cell growth in organ-on-a-chip devices. The latest published reports that use this method to find the TEER measurements conclude a large variation in same and different cell line studies. The current study was motivated to find an efficient method to monitor and study the cell growth in the chip system. Indeed, the transcellular-paracellular circuit was used with considerable changes to reduce the large variations shown in literature.

CHAPTER 1

INTRODUCTION

1.1 Placenta

The human placenta is a temporary organ that is created during pregnancy. The placenta connects and separates the mother and the conceptus to allow nutrient and metabolic waste transportation, gas exchange, and hormone creation to support pregnancy. The placenta can also create hormones to fight against internal infections caused by xenobiotics, bacteria, viruses, and parasites. During pregnancy, mother and fetus may interfere with various toxics that could be harmful for both mother and fetus.[1] Alcohol, drugs, and tobacco use can significantly impact the chance of getting chemical compounds which may harmful as well.[2] Toxics and chemical compounds could cause placental function failures under main functions such as the hormone production and release, and nutrient/metabolic waste transport.[3] Also, this could affect the growth of the conceptus from the prenatal beginning stage to the delivery stage. Substance transportation from mother to fetus occurs through a multilayered structure called "placental barrier".[4] This two-way transportation of nutrients, oxygen, and metabolic waste could get blocked and cause significant damages to the health of both mother and fetus. Even though the placenta is supposed to fight against these types of infections, it is clear that interfering substances can cross the placental barrier and cause developmental toxicity.

1.2 Placenta-on-a-chip

Researchers have conducted a wide range of different studies on placental transport including *in vivo* and *ex vivo* animal models. These animal models provided inconsistent results

as well as inaccurate predictions due to differences in physiological functions in human and animal models. In some studies, antibiotics and hormones were used to experiment the placental transfer in humans.[4] This particular type of study is always hard to perform due to the risk of exposure to the fetus. This is one of the main reasons as to why the placenta is the least understood human organ. Therefore, researchers changed their direction of placenta experiments toward the "Organ-on-a chip" technology.

1.3 Trans-epithelial electrical resistance (TEER)

Trans-epithelial electrical resistance (TEER) is an efficient parameter to monitor and study the cell growth in chip systems.[5] Previous studies have been conducted using direct current (DC) measurements to study the TEER in Organ-on-chip technology. Previous studies conducted using this method provide conflicting results; differences are unexplainable when the results are compared to conventional Transwell systems with microfluidic systems. Odijk et al.[5] provided a mathematical model that can be used to measure the TEER between microfluidic chips and Transwell cultures. This study was conducted to measure the TEER in two different geometries: microfluidics chips and Transwell cultures. In past studies, EVOM2 and a similar Millicell ERS-2 are used with Ag/AgCl electrodes to measure the TEER. Millicell ERS-2 or similar instruments are comparatively expensive and it is something not necessary to purchase for just one experiment. In this study, industrial multimeter is used with Ag/AgCl electrodes to make the path of conducting under easy and low-cost system to measure the TEER.

1.4 Objectives

The objective of designing a placenta-on-a-chip is to provide a more accurate drug testing model to study drug delivery to the placenta. This model will eliminate the need of animal models to test drugs. The objective for the TEER experiment is to use a multimeter to measure all TEER measurements in the placenta-on-a-chip device. The main goal is to compare the results using both theoretical and experimental methods.

1.5 Outline

A summary of next chapters are as follows:

Chapter 2**:** Literature review on different *in vivo* animal drug testing, *ex vivo* animal drug testing and placenta-on-a-chip designs.

Chapter 3**:** Placenta-on-a-chip design factors, final design and fabrication techniques are discussed.

Chapter 4**:** Cell culturing techniques are discussed in detail. Cell injecting procedure to the chip explained.

Chapter 5**:** TEER model for both theoretical and experimental methods are discussed.

Chapter 6**:** Results for the placenta-on-a-chip is discussed. TEER measurements from both theoretical and experimental methods are compared.

Chapter 7**:** Conclusions and future work are presented for each experiment.

1.6 References

1. Myllynen, P., M. Pasanen, et al. (2005). "Human placenta: a human organ for developmental toxicology research and biomonitoring." Placenta 26(5): 361-371.

2. Rockville (MD),Center for Substance Abuse Treatment. Substance Abuse Treatment: Addressing the Specific Needs of Women. Substance Abuse and Mental Health Services Administration (US); 2009. (Treatment Improvement Protocol (TIP) Series, No. 51.)

3. Vähäkangas, K. and Myllynen, P. (2009), Drug transporters in the human blood-placental barrier. British Journal of Pharmacology, 158: 665–678.

4. Lee, J. S., R. Romero, et al. (2016). "Placenta-on-a-chip: a novel platform to study the biology of the human placenta." The Journal of Maternal-Fetal & Neonatal Medicine 29(7): 1046-1054.

5. Odijk, M., A. D. van der Meer, et al. (2015). "Measuring direct current trans-epithelial electrical resistance in organ-on-a-chip microsystems." Lab on a Chip 15(3): 745-752.

CHAPTER 2

ROAD TO PLACENTA-ON-A-CHIP

2.1 Microfluidics

Microfluidics is an area of research concerned with the design, manufacture, and formulation of engineering fluids at submillimeter scales (microliters or nanoliters). In the beginning, microfluidics was used in order to build precisely manipulatable microscale devices. Microfluidics was first used in semiconductor industry and later was expanded to micro-electromechanical systems (MEMS).[1] Microfluidic devices are commonly referred to as lab-on-chip technology.[1] Lab-on-chip technology is mainly used for biomedical research purposes. A primary goal of current research is to develop microfluidics technology to make the biomedical researchers' work easier than the current status. In the prevailing world, many microfluidic devices have been designed to represent the human organ research, but most of the devices failed to enhance the capabilities of the full organ. Although most of the microfluidic devices are made to represent everyday biomedical research, most of the designed microfluidic devices are still in the engineering phase. Any technology can be engineered with an appreciable degree of precision and ingenuity, however, identifying suitable application(s) is in itself a challenging task.

Engineers are having difficulties in building working models of microfluidic devices to present a micro-scaled function. So these devices are still in the development phase. Microfluidic devices cannot be easily designed by scaling-down a larger device, it requires significant modifications to the system. A few important concepts are defined below for describing a microfluidic device:

- Laminar versus turbulent flow: In microfluidic devices, the Re (Reynolds number) is in the laminar flow regime.

- Surface and interfacial tension: Liquids have the ability to reduce free energy by contracting the surface-air interface.[1] This is due to the higher surface tension between liquid molecules than between the liquid molecules and air interface. This phenomenon can be used to transport fluids through microchannels.

- Capillary forces: Capillary force or capillary action is often defined as the ability for fluid to move without assistance of or opposition from external forces like gravity. Because of this ability, tubing and microchannels in microfluidic devices have the ability to flow the liquid without any effects of external forces.

2.2 Organ-on-a-chip devices

Organ-on-chips are microfluidic devices designed to represent the physiological functions of tissues and organs by using living cells.[2] These chips have the ability to contain cells that can be cultured with continuous perfusion inside a micro-sized chamber on the chip designed to represent a specific tissue and organ. The simplest design with a single cell layer cultured onto a microfluidic flat-form can be developed into a complex microfluidic organ-on-chip model by using multiple cell layers separated by a membrane (representing the barrier between two tissues).

2.3 Why is a microfluidic platform appropriate to model an organ?

Microfluidic platforms used for Organ-on-a-chip applications are compartmentalized, thus mimicking organ structure.[3] Scaling laws create conditions favorable to mimicking organ-like environments on the scale in which interactions take place in these compartments. At this small scale, the concentration of secreted signaling molecules could reach those found in *in vivo*.[4] Furthermore, the confined nature of the compartments allows gradients of soluble molecules to be maintained as found in organs *in vivo*.[5] Furthermore, subcompartments could be created inside the channel due to laminar flow. In addition, disease conditions could be replicated inside an organ on a microfluidic chip with compartments by varying the fluid flowing through.

The presence of a number of compartments in the same chip allows it to maintain multiple well-regulated chemical and physical culture conditions. This is important in mimicking organ function because an organ contains multiple cell types that function separately but communicating with each to behave as one integrated system. Thus, the microfluidic approach with separate compartments helps in understanding cellular communication among cells and tissues.[6,7] The presence of spatially distinct, micro- scale compartments makes it possible to culture different representative cell groups under different chemical and physical parameters in order to model organ activity. Further, the ability to perform multiple 'experiments' on a small microfluidic chip makes the process cost effective and takes up less laboratory space. Parameters on the microfluidic chip can also be changed using valves to vary the conditions of the same structure.[8]

Since different tissues in an organ are analogous to different cell types in spatially separated compartments, it is possible to find further analogies in comparing tissue-tissue

interactions and cell group interactions on the chip. Mass and energy flow between compartments can be regulated to vary the soluble molecule and physical force transfer between tissues. Once these changes are induced, the resulting behavior of cell groups are observed in a device with a small footprint.[9]

Overall, complex organ level interactions can be created on a microfluidic chip. For example, the liver microenvironment was recreated *in vitro* on a PDMS microfluidic chip.[10]

2.4 Animal related placenta drug testing

Drug testing using animals can be divided into two categories: *in vivo* and *ex vivo.* In Latin, *in vivo* means "within the living" and *ex vivo* means "out of the living". In biological sciences, *in vivo* refers to experiments done in animals or humans as a whole organism while *ex vivo* refers to experiments conducted on an actual tissue outside of the whole organism. In *ex vivo* experiments, results are considered more accurate than *in vivo* experiments, as whole organism used in *in vivo* experiments are partially or completely dead during the experiment due to limited control on the living object. But in *ex vivo* experiments, there is more ability to control the conditions to represent the same functionality as the actual organ, but it is considered to be more difficult to compare with *in vivo* experiments. Section 2.4 is focused on *in vivo* and *ex vivo* placenta related experiments on animals.

2.4.1 *In vivo* placenta drug testing on animals

Placental transport was studied mostly using *in vivo* animal models. In 1977, Pedro Rosso conducted his research on "Maternal-Fetal Exchange during Malnutrition in the Rat''.[11] The main goal of this study was to monitor placental transfer of "α-amino Isobutyric acid". Three-day

pregnant rats were initially taken and fed with ad libitum (a stock diet) for two days. Rats were divided into two groups after the sixth day; an experimental and a control group were fed with two different percentages of casein diet. The transfer of α-amino Isobutyric acid was studied on day 20 and day 21. One placenta and one fetus from a rat of each group were removed to study the transfer of amino acid. Study showed that, the low casein fed rats had a smaller percentage of α-amino isobutyric acid in the fetus relative to the high casein fed rats. In another study published by Pedro Rosso in 1997, he studied the placental glucose transfer.[12] The same procedures were performed until day 20 of pregnancy. At day 21 of pregnancy, the rats were injected with urethane (200mg/100g of body weight). Then their left femoral vein was injected with pyranoside (1μCi/100 g of body weight) and after ten minutes, their right femoral vein was also injected with pyranoside (5 1μCi/100 g of body weight). Ten minutes after each pyranoside injection, maternal blood samples were taken to determine the glucose percentage. Low casein fed rats had a lower glucose percentage in their fetus' relative to the high casein fed rats.

Rosso et al. (1981) performed a study to determine the placental blood flow and nutrient transfer in different sized pregnant Guinea pigs.[13] Different aged guinea pig fetuses were divided into three groups relative to the body weight: small, average, and large. The goal of the study was to determine the transfer of α-amino isobutyrate and methylglucose with placental blood flow in the maternal side. The study concluded that the fetal growth retardation in guinea pigs was related to the low placental blood flow and smaller placenta. In this study, the placental mass was related to the body weight and three fetal sizes were determined by the body weight of the guinea pig dams. Strong correlations were found in α-amino isobutyrate transfer rates and smaller fetuses. This suggested that the fetal growth rate also depended on the availability of amino acids. In addition, the reduced transfer of α-amino isobutyrate and methylglucose is

relative to the fetal growth retardation in smaller fetus. Persson et al. in 1990 studied glucose and amino acid transfer in guinea pigs with intrauterine growth retardation and concluded that the reduction of placental blood flow was affected by the transfer of α-amino nitrogen to the fetus.[14] In addition, the intrauterine growth retardation was related to the 'fetal weight/placental blood flow' ratio. This is found to be a characteristic of human intrauterine growth retardation.[15] The change of 'fetal weight/placental blood flow' ratio is likely due a chromosomal abnormality or an intrauterine infection.

A study was performed by Osgerby et al., 2004 to determine how maternal undernutrition affects placental growth.[16] Birthweight is correlated with the fetal growth and the placenta grows proportionately with the fetus. Ewes were chosen to perform this study because they have a cotyledonary placenta in which fetomaternal exchange occurs at discrete locations. This study was performed on 48 ewes to determine the effects of maternal undernutrition on placental growth. Ewes were left under different nutrient conditions for 45, 90, and 135 days to get the test results. The results showed that placental weight on 45 and 90 days, which relatively reduced the insulin-like growth factor binding protein. In addition, the placentome number (number of fetal and maternal tissues involved) was found to not be affected by undernutrition or gestational age.

Another factor for intrauterine growth retardation is the low protein supply to the fetus. How the low protein supply affects intrauterine growth was studied by Malandro et al. in 1996 using rats.[17] Researchers have found that the intrauterine growth retardation also affects health after birth. A child born from the condition of intrauterine growth retardation has a higher risk of interfacing with coronary artery disease, stroke. Another study was performed on amino acid transport in the rat placentae of dams maintained with an adequate, low protein calorie diet. Maternal, fetal, and placental weights were controlled by the protein supply in amino acid

transport's control. Researchers have found that dams fed with a low-protein isocaloric diet had less maternal, fetal, and placental weights compared to dams fed with a 20% casein diet. This was mainly due to a decrease in "fetomaternal serum amino acid ratios". Nutrient transfer to the fetus was reduced due to this decrease in fetomaternal serum amino acid level.

Reid et al. (1999) performed a study to determine the effect of intrauterine growth retardation on glucose transporter proteins in rat fetuses with a gestation age of 19 days.[18] To study glucose transport (glucose transporter protein 1 and glucose transporter protein 2), maternal rats were killed and the uteri and fetuses removed. Western blotting and immunohistochemical analyses were performed in placental membranes to evaluate the densities of glucose transporter protein 1 and glucose transporter protein 2. It was found that intrauterine growth retardation had no effect on the amount of fetal glucose transporter protein 1 and glucose transporter protein 2 messenger ribonucleic acid. Loutsevitch et al. (2007) performed a study on baboons, which showed that moderate maternal nutrient restriction leads to placental morphological changes.[19] Poor nutrient supply to the fetus can result not only in intrauterine growth retardation of the fetus, but also effects on the mother. The basic reasons for poor nutrient supply come from the mother's side, including eating disorders, adolescent pregnancy, and nausea. Good fetal growth and good pregnancy outcomes are associated with a well-being of the placenta. Due to the similarities on the placenta structure of baboons and humans as well as human placentation, baboon models are widely used for placental drug testing. This study concluded that the low nutrient supply caused no change on the volumetric structure of the placenta, but at the end of the gestation, placental weight decreased without changing the fetal weight or length.

Coan et al. (2008) conducted a study to investigate how the placental nutrient transfer affects the placental efficiency (grams of fetus produced per gram of placenta) in mice.[20] The major determinant of fetal growth is the nutrient supply, which depends on the size, blood flow, and transporter efficiency of the placenta. Most research focused on the effects of reducing placental weight demonstrated failures in physiological functions. Human placenta studies have linked physiological function failures with disease risk after birth. Coan et al. concluded that the lower weight of placenta resulted in higher performance of amino acid transport in the placenta with this adaptation increasing age.[20]

Coan et al. (2010) performed an investigation on how the placental phenotype supports fetal growth in pregnant mice.[21] Low birth weight, low life expectancy, and low fetal growth are the results of undernutrition during pregnancy. Poor nutrition during prenatal development caused low birth weight. One hundred and thirty six virgin female mice were used to perform the study. After being housed with males, they were moved to a single house and fed with a low nutrition diet. On day three, mice were randomly selected and fed 80% of controlled diet supply. Then they were kept in a 12h dark light cycle with free access to water. The results showed that the both placental and fetal weights were reduced in the diet-controlled mice.

2.4.2 *Ex vivo* placental drug testing models on animals

A research paper published in 1996 by Polliotti et al. group developed an improved method for placental lobule long-term perfusion to investigate infection agents such as HIV (Human Immunodeficiency Virus) in maternofetal transfer.[22] Prior to this study, researchers were not able to continue the perfusion for more than 24 hours with fully functional placental lobule in order to study how agents were transferred from the maternal circulation. The main

problem of tissue contamination was solved with modifications to the perfusion conditions (i.e., improvement in oxygenation) including the use of a biohazard hood and an intravenous bag for the medium perfused in closed circuit. An oxygenator with Mera Silox-S 0.3 membrane and Electromedic Cardioplegia heat exchangers were used to provide more oxygen and a warm perfusate before the oxygenation.[22] The main parameters compared using this system were glucose consumption, lactate production, and hPL (human placental lactogen) production as a function of perfusion time. Glucose concentration, lactic acid levels, and hPL in the perfusate were measured using a Hitachi 717 analyser, Abbott TDX/FLX analyzer, and ELISA kit (Enzyme Linked Immunosorbent assay), respectively.[22] Experimentally measured data was compared with the theoretically calculated data for each four hour period on a concentration basis. To test an infectious agent such as HIV, the experiment was conducted in a laminar flow hood with safety precautions, as there is risk to researchers of contamination from the system. It was found that the newly introduced oxygenator and heat exchangers provided more temperature control and gas exchange and conserved more physiological functions in human placenta. Also, because it requires more than 24 hours to examine the course of an infection through a tissue, the system allowed testing of infection agents due to its long-term perfusion capability.

Woo et al. (2012) conducted the first study of how ochratoxin A (OTA) transfers in human placenta using perfused human placentae.[23] OTA analyses from animal related studies and human fetal samples were not yet able to establish how this mycotoxin transfers through human placenta because the physiological functions of human placenta differ with growth stages of growth and it is not accurate to make predictions from animal related studies due to differences between humans and the animal models. OTA transport through freshly obtained placentas (from 38-48 week, full term pregnancies) was studied in 4 hour periods. Towards full

term the thickness of placental cell layers decreases. Thus, the full-term placenta, with its decrease thickness of cell layers, might have allowed higher exposure of toxins to the fetus compared with less developed placentae. This study also found that the OTA transfer rate was much lower than for other micotoxins transported through the human placenta (ie: aflatoxin and Deoxynivalenol).[24]

2.5 Placenta-on-chips drug testing models

2.5.1 Placental barrier structure

The following information is based on "Multi-layered placental barrier structure integrated with microfluidic channels" by Miura et at. (2013).[25] The placenta separates the maternal and fetal flow and continuously monitors the substances transferred between maternal blood and fetal blood. The placental barrier consists of extracellular matrix and various types of cells, membrane matrices (ie: laminin and type IV collagen), and syncytiotrophoblasts. The syncytiotrophoblasts are a special type of epithelial cell, which are in direct contact with the maternal blood.[26]

2.5.1.1 Cell culture

HUVEC cells and BeWo cells were used to represent the endothelial cell layer and trophoblastic cell layer, respectively. HUVEC cells were obtained from Lonza and cultured with EGM-2 (Lonza) medium to get $5x10^5$ cells. BeWo cells were cultured in an F-12 Hams (Sigma) mixture containing 10% fetal bovine serum to get $7x10^5$ cells.

2.5.1.2 Chip fabrication and cell deposition

An SU-8 mold from photolithography was used to fabricate microfluidic channels onto the PDMS sheets. Both channels are 2 mm wide by 20 mm long. Two PDMS layers were sandwiched with a vitrified collagen membrane in between; the chip was assembled using acrylic boards and nuts.

HUVEC cells were placed onto the collagen vitrigel. After five hours of cell adhesion, the chip was flipped and BeWo cells were placed onto the other side of the collagen. After two days of cell culture, membrane-like matrices such as laminin and type IV collagen were observed and cells were identified using florescent imaging. This study was designed to create a 3D multilayered structure representing a basic structural placental barrier**.**

2.5.2 Placenta-on-a-chip

The following information is based on "Placenta-on-a-chip: a novel platform to study the biology of the human placenta" by Lee et at. (2015).[27] This study created a model to represent functions of the placenta using microfluidics and microfabrication. Placenta-derived human cells were used to recapitulate the functions of placenta organ by proposing a "Placenta-on-a-Chip" model, which can represent the perfusion of human trophoblast and human umbilical vein endothelial cells. The placental barrier was represented by a thin ECM membrane *in vitro* conditions.

2.5.2.1 Chip fabrication

Two PDMS layers were created with a microchannel on each layer, representing the top and bottom cell layers using a soft lithography technique. A negative photoresist, spin-coated

wafer was baked at 65^0C for seven minutes and at 90^0C for 40 minutes. Again the wafer was baked at 65^0C for five minutes and at 90^0C for 18 minutes, after placing the mask film with channel patter while exposing to UV (ultraviolet) light. Unexposed photoresist was removed by rinsing the baked layer with the developer solution and isopropyl alcohol. PDMS prepolymer was mixed with curing agent at a 10:1 weight ratio, poured onto the channel mold created on the silicon wafer, incubated for four hours at 65^0C, then placed in a vacuum chamber. Fully cured PDMS on the mold was separated and cut into a desired shape saving space for the microchannel. Collagen type I from BD Biosciences was mixed with an equal amount of distilled water and 10x DMEM to a final concentration of 2.43mg ml^{-1} and final pH of 7.4. Gel was dispensed onto the bottom layer channel area and dried overnight at room temperature. Then the bottom layer and top layer were assembled after treating with the plasma cleaner. Silicon tubes were inserted into the inlets and outlets and the chips were sterilized by UV before cell seeding.

2.5.2.2 Cell seeding

Vitrified membrane was coated with 40 µg ml^{-1} fibronectin and 1.5% gelatin solution to promote cell adhesion. After JEG-3 and HUVEC reached a cell density of 5 x 10^6 cells/ml, JEG-3 was first perfused to the bottom channel and sat inverted in the incubator for two hours. After two hours, HUVEC cells were perfused and the chip was incubated for two hours, inverted from the previous position. After two hours, medium perfusion was carried-out using a syringe pump at 30 µl/hr of volumetric flow rate for each cell layer (DMEM for JEG-3 and EGM-2 for HUVECs). Cells were cultured for three days with continuous flow of medium through the syringe pump. To study glucose transfer, DMEM was supplemented with 4.5 g/ml glucose and introduced to the bottom JEG-3 cell layer. After 68 hours of continuous medium perfusion, the

media were collected from the outlets the glucose concentration was measured. The study

concluded that microfluidic flatform was able to maintain cells alive for at least 68 hours.

2.6 References

1. Sackmann, E. K., A. L. Fulton, et al. (2014). "The present and future role of microfluidics in biomedical research." Nature **507**(7491): 181-189.

2. Bhatia, S. N. and D. E. Ingber (2014). "Microfluidic organs-on-chips." Nat Biotech **32**(8): 760-772.

3. Moraes, C., G. Mehta, et al. (2011). "Organs-on-a-Chip: A Focus on Compartmentalized Microdevices." Annals of Biomedical Engineering **40**(6): 1211-1227.

4. Torisawa, Y.-s., B. Mosadegh, et al. (2010). "Microfluidic platform for chemotaxis in gradients formed by CXCL12 source-sink cells." Integrative Biology **2**(11-12): 680-686.

5. Lecuit, T. and L. Le Goff (2007). "Orchestrating size and shape during morphogenesis." Nature **450**(7167): 189-192.

6. Moraes, C., Y. Sun, et al. (2011). "(Micro)managing the mechanical microenvironment." Integrative Biology **3**(10): 959-971.

7. Park, J. Y., S. Takayama, et al. (2010). "Regulating microenvironmental stimuli for stem cells and cancer cells using microsystems." Integrative Biology **2**(5-6): 229-240.

8. Song, J. W., W. Gu, et al. (2005). "Computer-Controlled Microcirculatory Support System for Endothelial Cell Culture and Shearing." Analytical Chemistry **77**(13): 3993-3999.

9. Bhatia, S. N. and D. E. Ingber (2014). "Microfluidic organs-on-chips." Nat Biotech **32**(8): 760-772.

10. Wagner, I., E.-M. Materne, et al. (2013). "A dynamic multi-organ-chip for long-term cultivation and substance testing proven by 3D human liver and skin tissue co-culture." Lab on a Chip **13**(18): 3538-3547.

11. Rosso P. (1977), "Maternal-fetal exchange during protein malnutrition in the rat. Placental transfer of alpha-amino isobutyric acid". J Nutr ;107:2002–5

12. Rosso P. (1977), "Maternal-fetal exchange during protein malnutrition in the rat. Placental transfer of glucose and a nonmetabolizable glucose analog". J Nutr ;107:20006–10.

13. Saintonge, J. and P. Rosso (1981). "Placental Blood Flow and Transfer of Nutrient Analogs in Large, Average, and Small Guinea Pig Littermates." Pediatr Res **15**(2): 152-156.

14. Jansson, T. and E. Persson (1990). "Placental Transfer of Glucose and Amino Acids in Intrauterine Growth Retardation: Studies with Substrate Analogs in the Awake Guinea Pig." Pediatr Res **28**(3): 203-208.

15. Nylund L, Lunell N-0, Lewander R, Sarby B 1983 Uteroplacental blood flow index in intrauterine growth retardation of fetal and maternal origin. Br J Obstet Gynaecol 90: 16-20

16. Osgerby, J., D. Wathes, et al. (2004). "The effect of maternal undernutrition on the placental growth trajectory and the uterine insulin-like growth factor axis in the pregnant ewe." Journal of Endocrinology **182**(1): 89-103.

17. Malandro MS, Beveridge MJ, Kilberg MS, Novak DA. Effect of low-protein diet-induced intrauterine growth retardation on rat placental amino acid transport. Am J Physiol 1996;271:C295–303.

18.   Reid, G. J., R. H. Lane, et al. (1999). "Placental expression of glucose transporter proteins 1 and 3 in growth-restricted fetal rats." American Journal of Obstetrics and Gynecology **180**(4): 1017-1023.

19. Schlabritz-Loutsevitch, N., B. Ballesteros, et al. (2007). "Moderate Maternal Nutrient Restriction, but not Glucocorticoid Administration, Leads to Placental Morphological Changes in the Baboon (Papio sp.)." Placenta **28**(8–9): 783-793.

20. Coan, P. M., E. Angiolini, et al. (2008). "Adaptations in placental nutrient transfer capacity to meet fetal growth demands depend on placental size in mice." The Journal of Physiology **586**(18): 4567-4576.

21. Coan, P. M., O. R. Vaughan, et al. (2010). "Adaptations in placental phenotype support fetal growth during undernutrition of pregnant mice." The Journal of Physiology **588**(3): 527-538.

22. Woo, C. S. J., H. Partanen, et al. (2012). "Fate of the teratogenic and carcinogenic ochratoxin A in human perfused placenta." Toxicology Letters **208**(1): 92-99.

23. Woo, C. S. J., H. Partanen, et al. (2012). "Fate of the teratogenic and carcinogenic ochratoxin A in human perfused placenta." Toxicology Letters **208**(1): 92-99.

24. Nielsen, J. K. S., A. C. Vikström, et al. (2011). "Deoxynivalenol transport across the human placental barrier." Food and Chemical Toxicology **49**(9): 2046-2052.

25. Miura, S.; Morimoto, Y.; Takeuchi, S.; Ieee, Multi-Layered Placental Barrier Structure Integrated with Microfluidic Channels. In *26th Ieee International Conference on Micro Electro Mechanical Systems*, Ieee: New York, 2013; pp 257-258.

26. Lee, J. S., R. Romero, et al. (2016). "Placenta-on-a-chip: a novel platform to study the biology of the human placenta." The Journal of Maternal-Fetal & Neonatal Medicine **29**(7): 1046-1054.

27. Lee, J. S., R. Romero, et al. (2016). "Placenta-on-a-chip: a novel platform to study the biology of the human placenta." The Journal of Maternal-Fetal & Neonatal Medicine 29(7): 1046-1054.

28. Caplin, J. D., et al. (2015). "Microfluidic Organ-on-a-Chip Technology for Advancement of Drug Development and Toxicology." Advanced Healthcare Materials **4**(10): 1426-1450.

CHAPTER 3

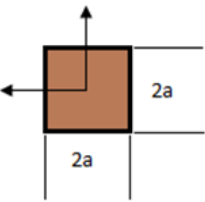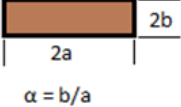# CHIP DESIGN AND FABRICATION

3.1 Chip design considerations

When determining the shape of the channels, three main factors were considered for accurate and efficient diffusion through the path: geometry of the cross-section, particle transport properties, and curvature of the flow path.

3.1.1 Geometry of the cross-section

Various shapes were considered when determining the cross-sectional geometry for the chip. Sharp et al.[1] summarized previous research work for flow through various cross-sectional geometries and compared how the Reynolds number (Re) and velocity would affect the flow through the channel. Due to the fact that every experiment on various cross-sectional geometries is conducted in a different range of Reynolds numbers and with different experimental conditions, it was hard to predict a relationship between the friction factor and the Reynolds number to compare different geometries. Different experiments with different parameters on the same cross-sectional geometry have also given different relationships to different factors. For example, in friction factors for different experiments that were conducted on the same cross-sectional geometry, there were some that followed the microscale predictions, some that gave higher values than predicted, and some that gave lower values than predicted. But for some parameter ranges, calculated friction factors in the flow of Newtonian fluid for channels with circular, rectangular, and trapezoidal cross-sectional shapes have given an agreement with the theoretical macroscale predictions. Sharp et al. concluded that parameters from the shape of the

cross-section create a relatively weak relationship with the Reynolds number and the velocity through the channel. **Table 1** shows a summary of the Reynolds number times the friction factor (f) and the ratio of maximum fluid velocity (u_{max}) to bulk velocity (u_B) for circular, square, and rectangular cross-sectional geometries.

Table 1: *Cross-sectional geometries of straight microchannel and their resistance to the flow* [1]

Cross Section	f Re	u_{max}/u_B
$D = 2a$ (circle)	64.00	2.0000
$2a \times 2a$ (square)	56.92	2.0962
$2a \times 2b$ (rectangle), $\alpha = b/a$	$96[1-1.3553\alpha + 1.9467\alpha^2 - 1.7012\alpha^3 + 0.9564\alpha^4 - 0.2537\alpha^5]$	-

3.1.2 Particle transport properties

     Particle transport properties were considered in determining the shape of the path. Bhagat et al. [2] conducted an investigation on how microparticles and nanoparticles passive filter in a microchannel with rectangular cross-sections. It was found that for solutions with low Reynolds numbers (Re < 50), travel through the rectangular cross-section would perform six equilibrium positions; three each on the broadest dimensions of the channel cross-section. In rectangular cross-sections, higher shear rates on the narrowest dimensions of the channel caused the particles

to move toward the longer channel walls by the resulting higher lift forces. An advantage of the rectangular cross-section is that the higher lift forces acting on narrow dimensions result in a shorter channel length being required for particle equilibration. According to the recent recorded data for channels with square cross-sections, the typical flows in microfluidic devices (Re < 50) cause eight stable equilibrium positions [3, 4]. This is due to the uniform shear gradient on all four sides of the square. In earlier studies, Segre and Silberberg [5, 6] provided a theoretical explanation of particle transport through a tube with a circular cross-section. According to Segre and Silberberg, uniformly distributed particles travelling through the tube will form a narrow band near the channel walls.

For the rectangular cross-section case, when it performs six stable equilibrium positions (three on each side) on the longer channel walls, one side of the longer channel wall interacts with the membrane on the design, which separates two channels. It is important to bring particles close to the wall next to the membrane, as this will create a higher percentage of the particles diffusing from one channel to another through the membrane. The simplicity of the rectangular cross-sections with straight side walls and no curves or bends on the walls makes it much easier to manufacture the channels. Because of those two reasons, we decided to choose a microchannel with a rectangular cross-section for the design.

3.1.3 Curvature of the flow path

After choosing the shape of the cross-section, it was important to make a decision about the curvature of the microchannel. Martel and Toner[7] conducted research to determine the effect of particle size and the channel curvature on particle migration in a channel with a rectangular cross-section. It was discovered that motion of the particles through a channel was controlled by

the main velocities caused by Dean Flow. Martel and Toner studied how the curvature of a channel controls the particle distribution and analyzed the effects of the curvature ratio on the distribution of different sized particles at constant Re_c. They found that with increased curvature ratio of the channel the Dean drag to the force equilibrium and shear lift were affected through redistribution of the velocity profile.[7]

Unbalanced forces on the particles cause their movement through the channels. The position of the particles will depend the on the size of the particles and the curvature of the channel. When the channel is straight, particles will remain on the long walls centered to the middle of the wall. When the curvature ratio of the channel increases, particles will move toward the center of the channel cross-section or to the narrowest geometry of the channel depending on the size of the particle. Having a curved channel design is not beneficial because, as the curvature increases, particles will start moving off the longer walls of the rectangular cross section. This will affect the interaction of the particles with the membrane in the design. When the particles are not interacting with one side of the longer wall, where the longer wall interacts with the membrane, it will cause a low percentage of the particles diffusing from one channel to another channel. It will also be too complicated to manufacture a channel designed to have a curvature. Therefore, a straight channel was chosen for the design.

3.2 Final chip design

Considering all above stated design factors, the chip was designed with straight channels and a rectangular cross-section. The two inlets and two outlets are separated with a 135^0 angle from the mid-section to make sure there is enough space to connect to the tubing (**Figure 1a).** The channel was designed with a width of 400 micron, a height of 10 micron, mid-section length

of 10 mm and inlet/outlet diameter of 1 mm. The two channels were separated by a membrane in the middle to represent the placental barrier (**Figure 1b).** Preparation of membrane will be discussed in a future section.
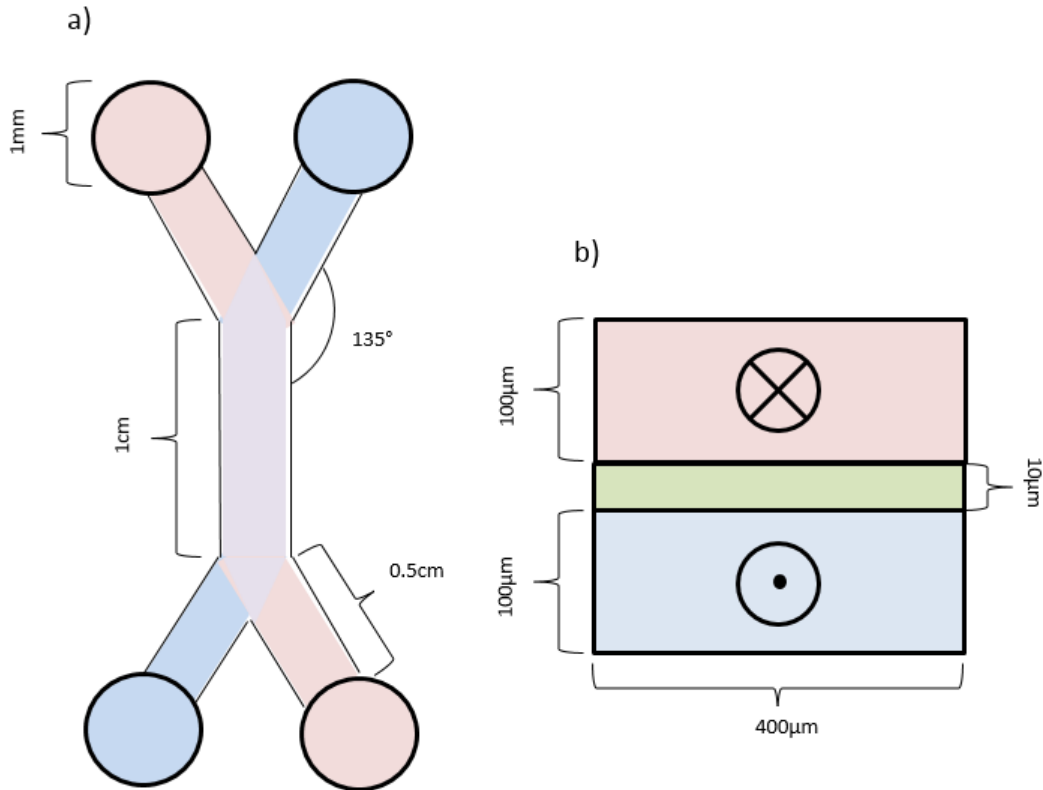

Figure 1: *Placenta-on-a-chip channel layout showing (a) aerial view of the top and the bottom channels with inlets and outlets, (b) cross-sectional view of the middle part of the chip containing two channels centered with the membrane. (not to scale) [8].*

3.3 Chip fabrication

Microfluidic chips are fabricated using a variety of materials. In this section, fabrication of placenta-on-a-chip using PMMA and PDMS is discussed.

3.3.1 Polymethyl Methacrylate (PMMA) fabrication

Initially, the placenta-on-a-chip was fabricated using PMMA. PMMA was chosen due to its clearness and ability of seeing through a microscope visually. A SolidWorks sketch is shown in **Figure 2,** was created as the first step of the placenta-on-a-chip fabrication.

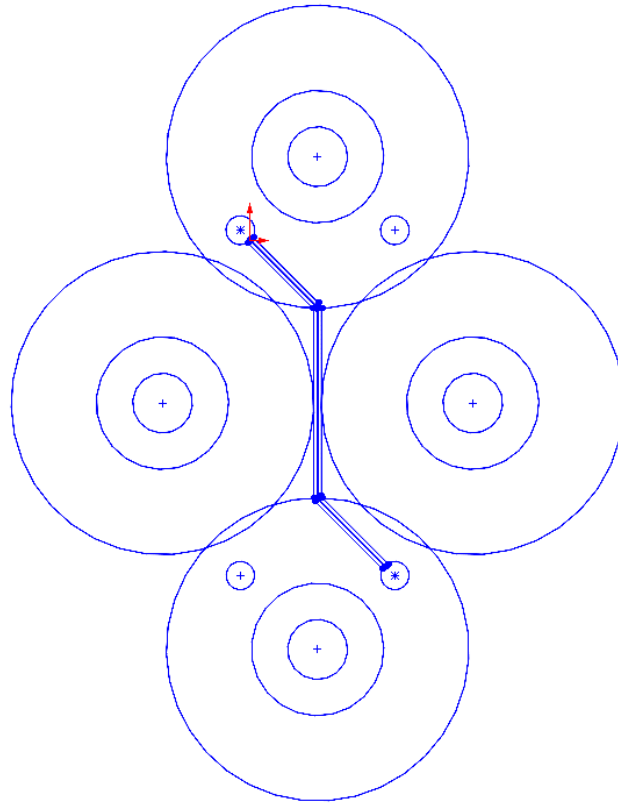**Figure 2:** *SolidWorks sketch of the placenta-on-a-chip for scale. Circles show the holes for screws and washers.*

A placenta-on-a-chip consists of two layers of PMMA separated by a thin polyester (PETE) membrane filter (0.4 micron pore-size; Sterlitech Corporation). The G-code was generated using the SolidWorks sketch and the two layers of the chip were milled using a CNC-Mini Mill-GX (Minitech Machinery).

Each channel of the microfluidic device was designed to have a cross-sectional width of 400 microns, a cross-sectional height of 100 microns, and a total channel length of 2cm. The same G-code was used to make holes for inlets and outlets and hole for the screws on the microfluidic device (**Figure 3a**). Each channel of the chip (**Figure 3b***)* was wiped with alcohol swabs for sterilization. Then both layers of the chip and the nuts, bolts, and washers were soaked for 20 minutes in a bath in 70% ethanol (**Figure 3c***)*.
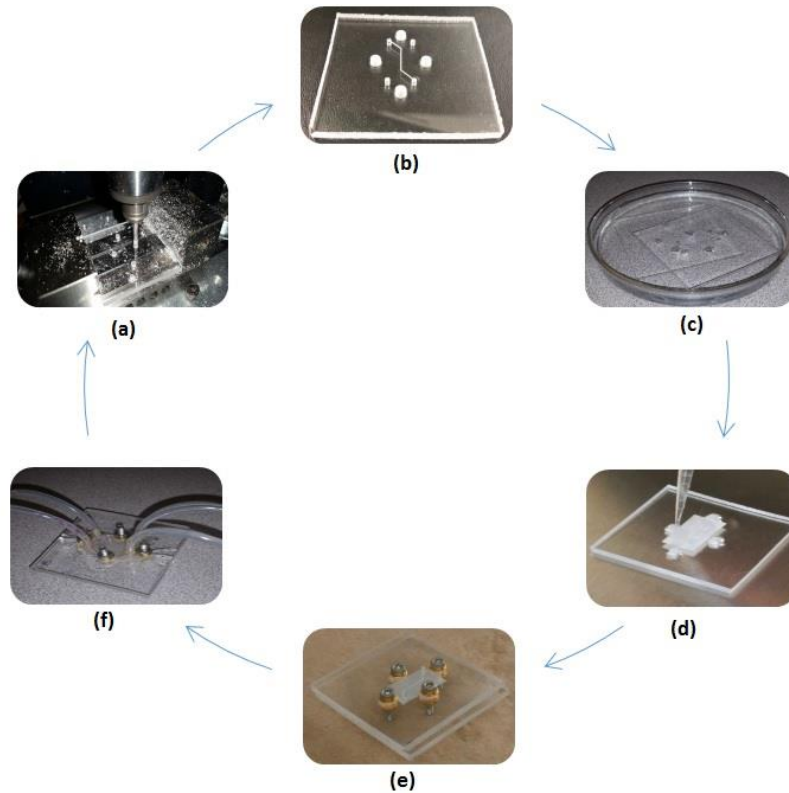
Figure 3: *The complete cycle of PMMA chip fabrication and assembly. (a) The PMMA workpiece was milled using the G-Code, (b) each channel on the completed PMMA layers was sterilized with ethanol swabs, and (c-f) the two layers were assembled with a gelatin-coated PETE membrane in between and tubing connected to inlets/outlets [9].*

1.5 % gelatin solution was prepared by mixing 1.5g of gelatin from porcine skin (Sigma-Alrich) with 100mL of ddH$_2$O. The solution was autoclaved for 20 minutes and cooled at room

temperature until the solution reached room temperature. A 70% ethanol-washed PETE

membrane piece was placed on the bottom layer of the chip covering the area of the section

overlapping the top and bottom channels (mid-section). Then the membrane was coated with 20

µL of prepared 1.5% gelatin solution as shown in **Figure 3d** (this process was done in a

biological safety cabinet). The layer with the gelatin coated membrane was incubated for two

hours before assembling. Two layers were sandwiched together and washers, nuts, and bolts

were inserted to hold them (**Figure 3e**). Nuts and bolts were tightened after aligning the top and

bottom channels with the aid of a microscope. Four small 1/16 ft. diameter PEEK tubes (IDEX

Health and Science) were inserted to the inlets and outlets and attached to 0.062 x 0.125 inch

laboratory tubing (DOW Corning) with epoxy glue for a completed device (**Figure 3f**).

3.3.2 PDMS fabrication

This section will be focused on the technique used to create PDMS microfluidic devices.

Soft lithography technique is used to create silicon wafer molds, which will be used as a mold to

create the microfluidic devices. Then, soft lithography replication is used to create the PDMS

microfluidic devices using the silicon wafer mold. Section 3.3.2.1 and Section 3.3.2.2 are

focused on the PDMS soft lithography and PDMS soft lithography replication, respectively.

3.3.2.1 PDMS soft lithography

Different researchers use different steps for soft lithography to create microfluidic

devices. In this section, one method of creating a silicon wafer mold using soft lithography

technique is explained.

The first step is to clean a new wafer using piranha solution ($H_2SO_4 + H_2O_2$) or acetone. To allow the SU-8 coating to stick better, the wafer is heated for 15 minutes at 120^0C. The next step is to create a negative photoresist using a spin coating technique. This photoresist layer will later be the mold. The Su-8 negative photoresist is created in two steps: low rotational speed and acceleration for 10-30 seconds and high rotational speed and acceleration for 30 to 60 seconds to

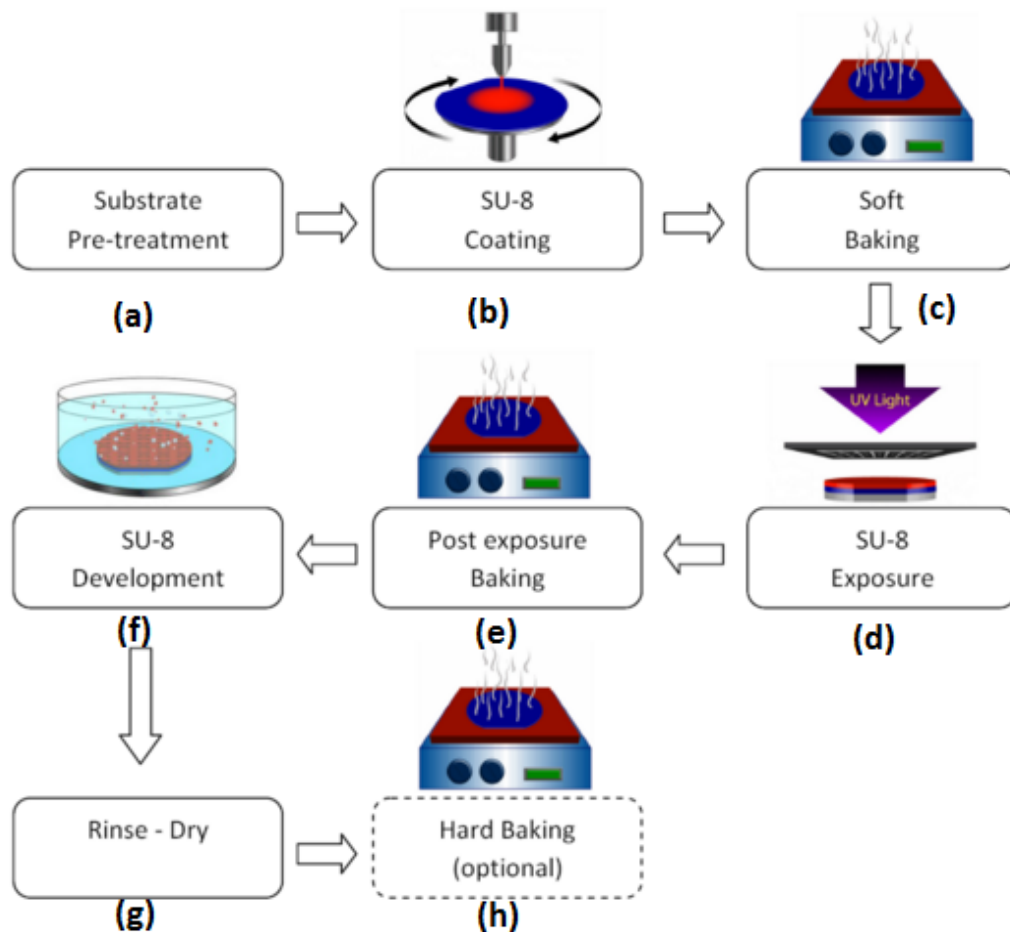**Figure 4:** *Eight step SU-8 mold fabrication process. The SU-8 coating is used for silicon wafer substrate. Eight steps are (a) preparation of the wafer, (b) spin coating of the negative SU-8 photoresist, (c) first bake the photoresist (soft bake), (d)UV exposure, (e) second bake the photoresist (post exposure bake), (f) SU-8 development, (g) rinse with isopropanol, and (h) third bake the photoresist (hard bake)* [10].

achieve a 100micron thick layer. To make the SU-8 photoresist more solid by evaporating the solvent, the wafer goes through the soft baking process. The soft baking process is broken into two steps: ten minutes at 65^0C and 30 minutes at 95^0C. After the baking process, a photoresist edge bead appears around the wafer due to surface tension from baking. To remove the edge bead, acetone is injected while the wafer is rotating at a high speed. UV exposure is used to initiate the cross linkage by the activation of PhotoActive component in the photoresist [10]. A layout of the "channels visible" photo mask is placed on the wafer, so that the part that is exposed by the UV light (channels) will harden. The exposure wavelength during the SU-8 hardening is 365 nm and the exposure energy is 480 mJ/cm^2. After the UV exposure, the wafer undergoes through the second photoresist bake. This will generate more energy to continue the PhotoActive reaction. The baking is done in two steps similar to the soft baking, but for different durations: one minute at 65^0C and ten minutes at 95^0C, continuously. When the wafer reached room temperature, the SU-8 developer solution was used to dissolve the non-linked SU-8 photoresists. Then the wafer was rinsed using isopropanol and left to dry. Afterwards, the third and final baking process was performed, which is an optional step that can prevent future cracks.

3.3.2.2 PDMS lithography replication from SU-8 mold

Polydimethylsiloxane (PDMS) is a polymer that is widely used to create microfluidic devices with SU-8 molds. PDMS is created by mixing a curing agent with PDMS at different w/w ratios depending how hard or soft the PDMS needs to be. Once the SU-8 mold was created, the PDMS solution was created by mixing the curing agent and the PDMS at 1:10 w/w for this research purpose. The created SU-8 mold was placed on a 15 cm diameter petri dish (relatively larger than commonly used) and ready to be used as the mold. Well-mixed PDMS was poured

into the petri dish containing the master mold and left on a balanced table for at least 24 hours before use. Once the PDMS solidified, it was cut around the substrate and peeled off the mold. After separating the layers into the designed shape, inlet/outlet holes were made using a puncher. To assemble the chip, pre-created vitrified collagen membrane (vitrified collagen membrane creation is discussed in next section) was placed on the bottom layer and both top and bottom layers were plasma cleaned. Plasma cleaning activates the Si-CH$_3$ surfaces to Si-OH so that, when surfaces are pressed against them, a strong and permanent Si-O-Si link is formed. [11] The chip was sterilized by leaving it under UV for 20 minutes.

3.3.2.3 Vitrified collagen membrane

PETE membranes with 0.4 micron diameter pores were obtained from Transwell plates with membrane inserts (Corning). Concentrated collagen from rat tail tendon (8.38 mg/mL) was obtained from Corning® and mixed with equal amounts of Dulbecco's MEM (10X) and de-ionized water to bring the collagen to a final concentration of 2.5 mg/mL. Both sides of PETE membranes were coated with the prepared collagen solution and left in the room temperature for six hours. Once the collagen dried on the membrane, they were used for the chip assembling process.

3.4 References

1. Sharp, K. V., Adrian, R.J., Santiago, J.G., and Molho, J.I., Liquid Flow in Microchannels. In *The Handbook of MEMS*, Gad-el-Hak, M., Ed. CRC Press: Boca Raton, Florida, 2001; pp 1-45.
2. Bhagat, A. A. S., S. S. Kuntaegowdanahalli, et al. (2008). "Enhanced particle filtration in straight microchannels using shear-modulated inertial migration." Physics of Fluids **20**(10): 101702.

3. Chun, B. and A. J. C. Ladd (2006). "Inertial migration of neutrally buoyant particles in a square duct: An investigation of multiple equilibrium positions." Physics of Fluids **18**(3): 031704.

4. Kim, Y. and Yoo, J., "The lateral migration of neutrally-buoyant spheres transported through square microchannels," J. Micromech. Microeng. 18, 065015 (2008).

5. Segre, G. and Silberberg, A., "Behaviour of macroscopic rigid spheres in Poiseuille flow," J. Fluid Mech. 14, 136 (1962).

6. Segre, G. and A. Silberberg (1961). "Radial Particle Displacements in Poiseuille Flow of Suspensions." Nature **189**(4760): 209-210.

7. Martel, J. M. and M. Toner (2013). "Particle Focusing in Curved Microfluidic Channels." Scientific Reports **3**: 3340.

8. Jeremy Caplin, Catherine Meis and Nastaran Hashemi, "Utilizing Microfluidic Technology to Replicate Placental Functions in a Drug Testing Model" ASME 2015 4th Global Congress on NanoEngineering for Medicine and Biology, Minneapolis, MN, April 19-22, 2015.

9. Norma Granados, Rajeendra Pemathilaka, Lindsey Matheney, Jeremy Caplin, Marta Sucur and Nastaran Hashemi, "Microfluidic drug Testing Placenta-on-a-chip Device" Iowa Illinois Nebraska STEM Partnership for Innovation in Research & Education, Ames, Iowa, July 07, 2015.

10. Elveflow. (2015). The SU-8 mold fabrication process: Tips and tricks. Retrieved February 20, 2016.

11. Elveflow. (2015). The SU-8 mold fabrication process: Tips and tricks. Retrieved February 20, 2016.

CHAPTER 4

PLACENTA-ON-A-CHIP

In this chapter, HUVEC and BeWo cell culturing techniques and placenta-on-a-chip

testing procedures are discussed. Section **5.1** is focused on the cell culturing. Most parts of the

processes are followed according to the original manufactures' protocols (Lonza and ATCC) [1, 2].

4.1 Cell culture

4.1.1 HUVEC cell culturing

The base medium used for HUVEC cell culturing is EBM-2 (Endothelial Basal Medium)

from Lonza. EGM-2 (Endothelial cell growth medium) was created by mixing the SingleQuots

Kit with the basal medium. The SingleQuots Kit contains cytokines, growth factors, and other

supplements.

4.1.1.1 Starting and maintaining an original HUVEC cell vial

The original HUVEC cell vials were stored at $\sim$ -200^{0}C in liquid nitrogen. First, 10mL of

EGM-2 in a T-75 cell culture grade flask was left in an incubator at 37^{0}C with 5% CO_2 for 20

minutes. Once the medium in the flask was ready, a cell vial was removed out from the liquid

nitrogen freezing unit and thawed in a 37^{0}C water bath for a few seconds until the ice could be

barely seen at the bottom of the vial. Then the contents of the vial were transferred into the T-75

flask and the flask was placed inside the incubator.

The medium was changed 24 hours after seeding and every 48 hours thereafter.

Following the HUVEC culture manual in Lonza, the volume of medium depended on the cell

confluency in the flask. If the percent of confluency was 45% or higher, the media volume was increased by 4-5mL of medium that had been thawed in a 37^0C water bath for 20 minutes before refreshing media.

4.1.1.2 Subculturing HUVEC Cells

Cells are ready for the subculture once they have reach 70-85% of confluency. Trypsin/EDTA solution was used as the dissociation solution. First, old media was removed from the T-75 and the attached cells were rinsed with 3 mL of 0.025% (w/v) trypsin in 0.01% EDTA solution (Gibco®). Then 2ml of trypsin was introduced and left over the cells and the flask left at room temperature for about 15 minutes. Over this time period the flask was observed couple of times under the microscope to check for cell detachment. Trypsin should not be left on the cells for more than 20 minutes as it can destroy them. Once most of the cells were detached the trypsin solution containing the cells was placed into a 15mL conical tube that was then filled with EGM-2 up to 10mL. The cells were centrifuged at 200 x g for five minutes and the medium was removed from the conical tube. The pellet was used for freezing the cells or their subculture. Since the cells are really expensive, it is important keep a backup storage of frozen cells for future use. The most important part of the freezing the cells is the composition of the freezing medium. For most cell types the freezing medium contains 10% DMSO (dimethyl sulfoxide) and 90% complete medium. For HUVECs, it is 10% DMSO and 90% of EGM-2. To freeze cells in a pellet, about 3mL of EGM-2, 10% DMSO was added to the conical tube and medium was mixed with the pellet using a micropipette. One milliliter was transferred to each cryovial, which were left overnight in a -80^0C freezer and then transferred to liquid nitrogen storage.

Cells were subcultured at a dilution ratio of 1:3 as follows. 10mL of EGM-2 was transferred to a T-75 flask and incubated for 20 minutes. Once the medium was ready, equal amounts of the cells mixed with EGM-2 were transferred to three T-75 flasks, and the same medium refreshing procedures were followed as discussed in Section 4.1.1.1.

4.1.2 BeWo cell culturing

The base medium used for BeWo cell culturing was F-12K medium (Kaighn's Modification of Ham's F-12 Medium) from ATCC®. The complete growth medium was created by adding 10% of FBS (Fetal Bovine Serum) from ATCC® from the total volume of base medium (F-12K).

4.1.2.1 Starting and maintaining an original BeWo cell vial

A T-75 cell culture grade flask was filled with 10 mL of F-12K growth medium and incubated for 20 minutes at 37^0C and 5% CO_2. The original BeWo cell vial was removed from the ~-200^0C liquid nitrogen freezing unit and thawed in a 37^0C water bath for a few seconds until the ice at the bottom of the vial could barely be seen. Once the flask with medium was ready, cells from the vial were transferred to the flask using a micropipette. The flask was incubated for 24 hours.

After 24 hours of seeding, the flask was observed under the microscope to see if the cells were at 45% or higher of confluency. Then the flask was refreshed with F-12K growth medium and every 48 hours thereafter. The refreshing volume of the F-12K growth medium was increased by 3-4 mL, depending on the percent of confluency increase rate.

4.1.2.2 Subculturing BeWo Cells

Once the cells were at 70-85% of confluency, subculturing was performed following ATCC® protocols for BeWo cells. Firstly, the current medium in the flask was removed and discarded and the cell layer was rinsed with 3 mL of 0.025% (w/v) trypsin in 0.01% EDTA solution to remove all vestiges of serum from the flask. Trypsin EDTA solution (2-3 mL) was added to the flask and the cells observed under the microscope for 5-15 minutes until they were dissociated. As discussed in Section 4.1.1.2, trypsin should not be kept for more than the recommended time (15 minutes maximum for BeWo cells), as it will destroy the cells with extended period of time. Once most of the cells were detached, the harvested cells were transferred to a conical tube and filled with F-12K growth medium up to 10mL in total. Cells were then centrifuged at 250 x g for five minutes. Afterwards, medium was removed from the tube carefully and the pellet was mixed with about 30 mL of F-12K (if subculturing) or 3 mL of freezing medium (if freezing). As discussed in Section 4.1.1.2, the user has the choice of freezing cells or subculturing cells. Freezing medium was created using 5% of DMSO and 95% of F-12K growth medium. The same procedures were followed for cell freezing and subculturing, as discussed in Section 4.1.1.2.

4.2 Placenta-on-a-chip testing procedures

Placenta-on-a-chip testing procedures consisted of five main steps: staining cells, harvesting cells, controlling cell density, introducing cell lines, and maintaining cell lines in the channels.

4.2.1 Cell staining

Cell staining is a technique used to identify cells or cell components on a substratum. This section is focused on using CellTracker™ staining for both cell types: HUVEC and BeWo. Information is based on the CellTracker™ protocol for fluorescent probes [3]. For this experiment, CellTracker™ Green CMFDA and CellTracker™ Orange CMFDA (Life Technologies) short-term dyes were used for HUVEC and BeWo cells, respectively.

Firstly, the CellTracker™ fluorescent probe was allowed to warm to room temperature. Then the probe was diluted in DMSO (ATCC) to a final concentration of 10 mM. DMSO (10.76 µL and 9.08 µL, respectively) was added to HUVEC cells and BeWo cells. Afterwards, the
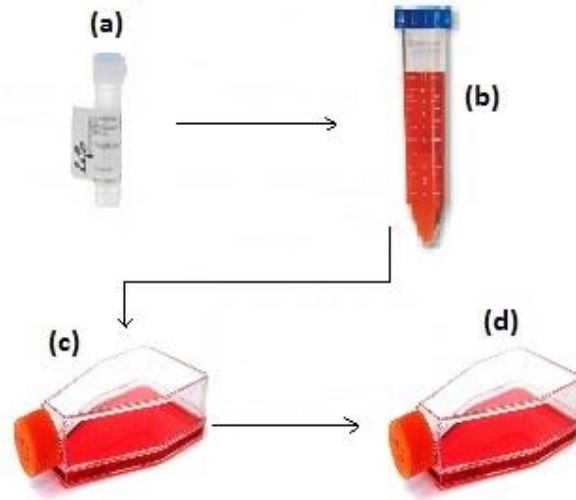

Figure 5: *Procedure to use CellTracker™ cell staining dyes for both HUVEC and BeWo cells. (a) Allow CellTracker to warm to room temperature, (b) dilute in DMSO and serum-free medium to a final concentration of 0.5-25 µM, (c) refresh the flask with pre-created CellTracker solution and incubate it for 15-45 minutes, and (d) refresh the flask with growth medium.*

solution was diluted in a serum-free medium (base medium) to a final working concentration of 0.5-25 µM. It was calculated that CellTracker Green for HUVEC could be diluted in 4 – 214 mL of EBM and CellTracker Orange could be diluted in 3 – 182 mL of F-12K base medium. CellTracker working solution was then warmed to 37^0C, which was subsequently used as a replacement for the growth medium. The flasks were incubated for 15-45 minutes (depending on the cell type) while containing CellTracker working solution. After incubation, CellTracker solution was removed and replaced with growth medium. The process of cell staining is shown in **Figure 5**.

Cells may take longer than 45 minutes to display some results, so it is better to incubate for another couple of hours before harvesting cells. Cell harvesting is discussed in the next section.

4.2.2 Harvesting cells

Cell harvesting from a T-75 flask is discussed in Section 4.1.1.2 in detail. **Figure 6** shows specific procedures of cell harvesting for the purpose of cell introduction to the placenta-on-a-chip. As discussed in previous section, a cell pellet was obtained after centrifuging. Depending on the size of the pellet, 100-300 µL of growth medium was introduced to the conical tube and mixed well with the cells by resuspending from a micropipette, then it was transferred to a cryovial. The amount of growth medium transferred to the conical tube is important, as a higher volume of growth medium mixed with a smaller pellet may result in too low a cell density. Procedures of controlling the cell density is discussed in next section.
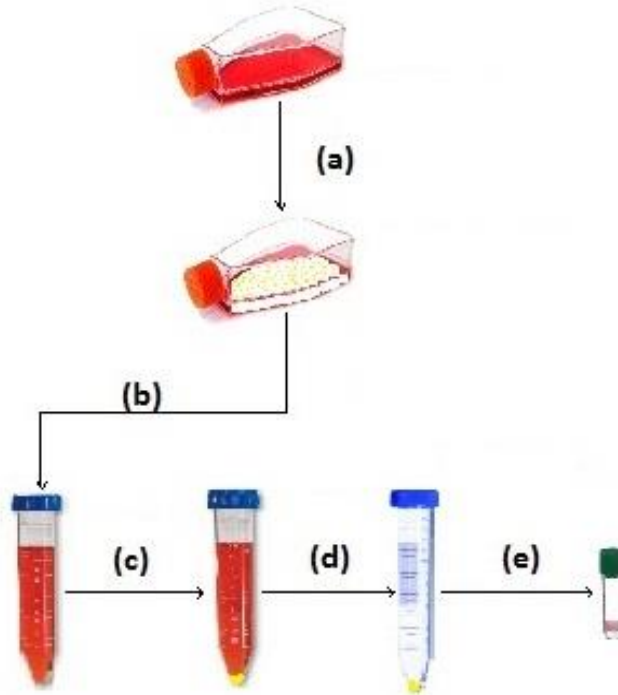
Figure 6: *Procedures for cell harvesting, (a) remove old medium and rinse the cell layer with 3mL of trypsin/EDTA solution. Introduce 2-3 mL of trypsin and allow for cell detachment, (b) after 15-20 minutes (depends on the cell type) transfer content to 15mL conical tube and fill with growth medium up to 10mL in total, (c) centrifuge for 5 min, (d) remove the medium, and (e) Add 200µL of medium and transfer into a cryovial. *The centrifuge is run at 200 x g and 250 x g for HUVEC and BeWo cells, respectively. The volume of medium for resuspension can be changed depending on the size of the pellet.*

4.2.3 Controlling cell density

It is important to make sure the suspended densities of both cell types are 5 x 10^6 cells/mL before being introduced to the chip. It was always assumed that the suspended cell density, which is determined by the volume of growth medium added to the cell pellet, should be higher than required. If the measured suspended cell density (as discussed in this section) is lower than 5 x 10^6 cells/mL, the cells should be centrifuged again and resuspended in a smaller

volume of growth medium. Assuming 200 µL of growth medium was mixed with the pellet, 10

µL of well mixed cells plus medium was transferred to a cryovial. Then 40 µL of trypan blue

solution (Gibco) was added and well mixed until the cells were uniformly suspended. Ten µL of

cell suspension was introduced into a grid on one side of a hemocytometer (LW Scientific) and

observed under the microscope. An image of the middle portion of a large square on the grid is

shown in **Figure 7.**

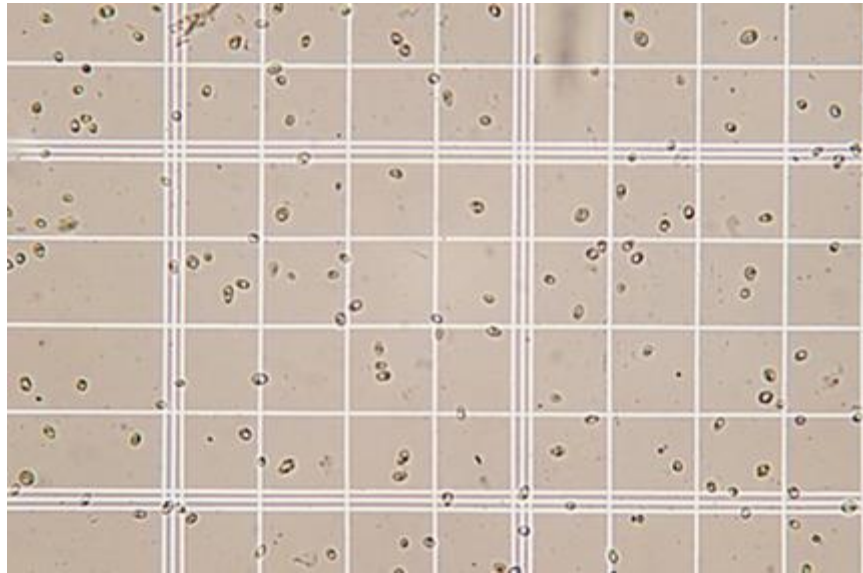   A hemocytometer is a counting chamber used to determine cell density. Usually,

Figure 7: *Cells mixed with Trypan Blue solution on Hemocytometer.*[4]

hemocytometers consist of two main grids, containing nine squares each. The central square

consists of 25 larger squares and each large square is divided into 16 smaller squares. Trypan

blue solution is an exclusion staining dye used to identify dead cells. When mixed with trypan

blue, dead cells appear blue. Once the cells were counted on the central square, the following

equation was used to calculate the density of live cells in the suspension.

$$Total\ cell\ density\ \left[\frac{cells}{mL}\right] = Total\ cells\ counted\ \times \frac{dilution\ factor}{\#\ of\ squares} \times 10,000\ \left[\frac{cells}{mL}\right]$$

After finding the density of suspended cells, the following equation was used to convert the current cell density to a desired suspended cell density.

$$\frac{V_1}{V_2} = \frac{\rho_1}{\rho_2}$$

Where V_1 and V_2 are the initial volume of the solution and the volume needed to add to the solution to get the desired cell density, respectively. ρ_1 is the initial cell density and ρ_2 is the desired cell density. Once the suspended cell densities are adjusted to 5×10^6 cells/mL, the cells are ready to be introduced to the chip.

4.2.4 Introducing and maintaining cells on the chip

PDMS chips created using the soft lithography replication technique (as described in Chapter 3) were sterilized under UV irradiation for 20 minutes. The HUVEC cells were injected to the top channel of an inverted chip using a micropipette and the chip was placed on a petri dish with a lid. Two to three small caps filled with autoclaved deionized-water were placed on the petri dish to provide humidity and control evaporation. The chip was incubated for 12 hours to allow for cell adhesion. After 12 hours, the chip was inverted and the BeWo cells were injected to the bottom channel of the chip and the chip was incubated for another 12 hours to allow cell adhesion. The evaporation was controlled by leaving EGM-2 and F-12K growth medium bubbles on top channel inlet/outlet holes and bottom channel inlet/outlet holes, respectively. After 24 hours of cell adhesion in total, the channels were observed under a microscope. Fluorescent images were taken following the ZEISS microscope protocols.

After fluorescent imaging, four small (1/16 ft. diam.) sterile PEEK tubes (IDEX Health and Science) were inserted into inlets and outlets and connected to a 0.062 x 0.125 inch laboratory tubing (DOW Corning). Then the inlet tubes were connected to 3mL syringes (Becton, Dickinson and Company) that were connected to a syringe pump (Kent Scientific).
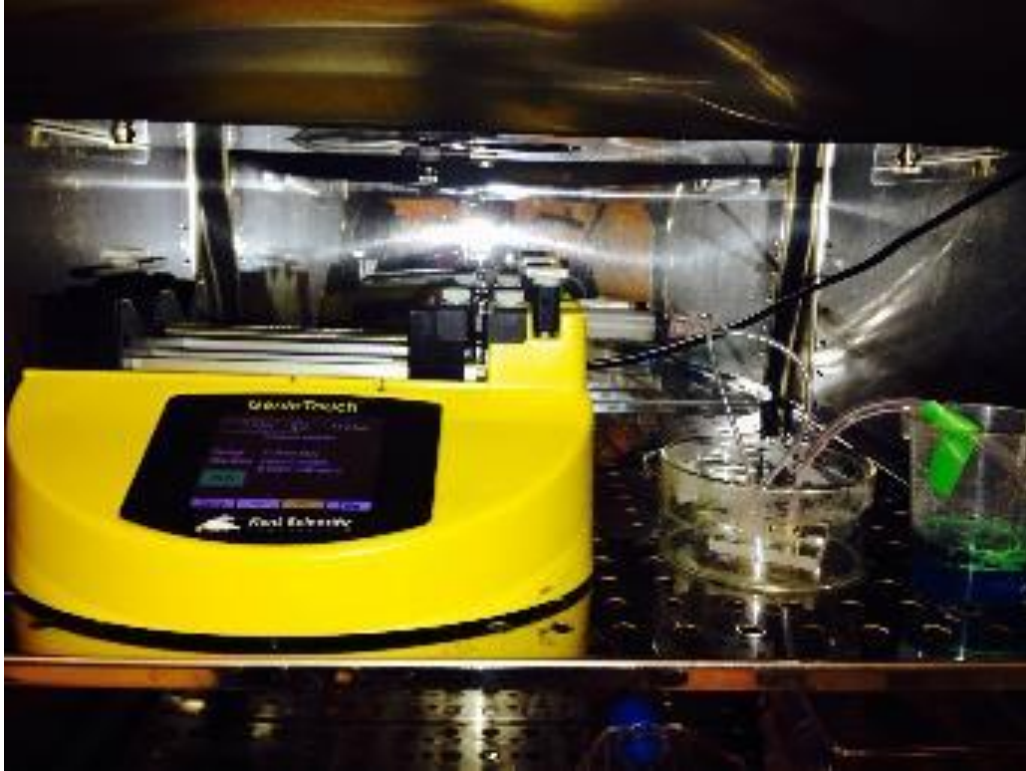

Figure 8: *Channel inlets connected to a syringe pump running at a constant volumetric flow-rate. Outlets were fed into a calcium chloride solution to kill cells.*

Outlet tubes were sent to a waste container consisting of 10 mM $CaCl_2$ (calcium chloride) when the set-up was running inside an incubator or 70% ethanol when the set-up was running outside an incubator. The microfluidic cultures were perfused at a constant volumetric flow rate of 1μL/min driven by 3 mL syringes filled with respective growth medium for each cell type. The schematic of this set-up is shown in **Figure 8**.

4.3 Reference

1. CloneticsTM Endothelial Cell System; Lonza Walkersville, Inc.: Walkersville, MD, 07/15, 2015.

2. BeWo (ATCC CCL-98TM) American Type Culture Collection: Manassas, VA, 06/01, 2013.

3. CellTracker^{TM} Fluorescent Probes (C2925 & C2927); Life Technologies; Thermo Fisher Scientific Inc.: Waltham, MA, 06/10, 2014.

4. DeLange, A.J. (2013). Hemocytometer. Retrieved April 02, 2016, from Wetnewf.org

CHAPTER 5

TRANSEPITHELIAL/TRANSENDOTHELIAL ELECTRICAL RESISTANCE (TEER)

IN MICROFLUDIC DEVICES

5.1 Introduction

TEER measurements (Transepithelial/ Transendothelial Electrical Resistance) are used as a quantitative method to monitor and describe the quality of the barrier function in epithelial and endothelial monolayers.[1] In microfluidic systems, TEER measurement conditions are different than for Transwell cultures due to three main reasons: smaller cell layer (only on the membrane of the chips), higher resistance due to the length of the channel, and different measurements depending on the method used.[5] Depending on the location of electrodes that measure the resistance along the membrane, the accuracy of the data can vary. When epithelial and endothelial cells are cultured to form a monolayer, they form tight intercellular junctions. These tight junctions can prevent free passage of ions and molecules through the intercellular space of a cell monolayer. The presence of tight junctions is characteristic of healthy, confluent monolayers of epithelial and endothelial cells. Various methods are described in the literature for making electrical measurements in chip devices. These include flow cytometry, patch clamping, electrophoresis and electrochemical detection.[6,7,8,9]

Cheung et al. (2005) conducted research to identify how flow cytometry can be used to characterize the cell population in a microfluidic channel.[6] In this study, the group used a "microfabricated impedance spectroscopy flow cytometer", where impedance was used to provide data such as size of cells, capacitance of membrane, and conductivity of cytoplasm. All the data was obtained as a function of frequency from dielectric measurements. One advantage

of using flow cytometry to distinguish cell populations is that it eliminates the need of externally added cell markers. Normally, in flow cytometry, cell separation is done by FACS (fluorescence activated cell sorting) or a DEP cross-over frequency-based (dielectrophoresis) technique, where at the frequency, the particles undergo zero dielectrophoresis force.[10] The "microfabricated impedance spectroscopy flow cytometer" is cost effective compared with DEP and FACS.[6] After analyzing the fabricated chips (platinum electrodes coated on two glass substrates) using microfabricated flow cytometer, it was found that the proposed method can be used to determine the properties of the membrane on which the cells are grown.[6]

Pantoja et al. (2004) used patch-clamp electrodes to analyze the macroscopic ion channel protein activities on a wafer-based microfluidic device.[7] The patch-clamping technique was invented to study ion channels and the effects of changing their physical and chemical surroundings. The original method of patch-clamping was done by using a 1-2 micron diameter pipette[11], but this method cannot be applied to a microfluidic system. To overcome this problem, Pantoja et al. proposed a wafer-based patch-clamping device to replace the traditional glass pipettes. In this study, they focused on the flow of the cells because, aligning the cells in the channel would allow them to analyze the macroscopic ion channel activities. They compared the results obtained with a traditional patch-clamped device with their proposed method and concluded that their method gave similar results to those obtained with the tradition patch-clamping method. They were able to record the current for 60% of any given cell type, but HIT-T15 cells were found to be the best compared to other cells used.[7] In summary, this group successfully made patch-clamping measurements using a microfluidic device connected to a voltage clamp setup to determine ion channel activities, as well and the conductance across cells attached to the voltage clamped membrane.

Lagally et al. (2000) conducted a study on protein and DNA separation by electrophoresis.[8] They created a microfluidic device capable of PCR (polymerase chain reaction) amplification of DNA. Their design allowed transfer of a small volume through the system and eliminated the need of manual load for the sample, which resulted in air bubbles during loading. Also, it eliminated the risk of contamination from the outside environment. They were able to produce 5-6 DNA copies before amplification. This was done by using fluorescent dye to detect the amplified product resulting from PCR amplification of only 20 DNA template copies/microliter. This method is considered to be more cost and time efficient than current methods.

These different techniques described in the literature require deposition of electrodes to analyze or monitor the quality of barrier function. An electrode deposition on substrates such as PDMS may result in low oxygen and carbon dioxide in the channels.[9] The limitation of oxygen and carbon dioxide may result in poor cell growth inside the system. Our chip is not designed to deposit electrodes. Therefore, the methods discussed above would not be beneficial. Also, depositing electrodes could cause serious damages to the chip, as well as PDMS chips loss in flexibility. Having electrodes above the membrane or in the area of the channel will affect the flow of the culture medium. Instead, a having electrodes inserted to the inlet/outlet will eliminate the need of touching the central membrane as well as limit damage to the cell layers.

5.2 Theory behind the TEER measurements

Two pathways are responsible for ion and molecular transport in cell monolayer: the transcellular pathway and the paracellular aqueous pathway. The transcellular pathway is the route that substance can pass through the cells [2]. This pathway describes the substances that pass

through an epithelial cell layer. The paracellular pathway describes the route that substances can

pass between the cells [3]. This includes substances passing through cell junctions as well as

intercellular spaces [4]. In younger cell cultures, the paracellular pathway plays a larger role in

TEER than the transcellular pathway, as the adhesion of the cells are not strong and cells have

not yet formed tight junctions. In this study, the endothelial cell barrier (tissue barrier) is

substituted with a simple circuit, with resistors that represent the charge carried by the substances
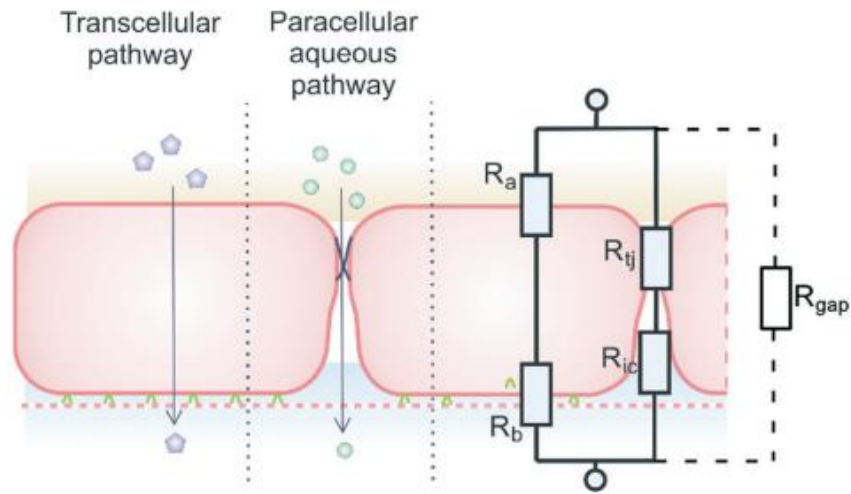

Figure 9: *Simple circuit representing an endothelial cell layer forming a barrier, original image based on Abbott et al [1, 5]. Reproduced from Odijk et al. [1] with permission of The Royal Society of Chemistry.*

passing through each pathway as shown in **Figure 9**. In **Figure 9**, the sum of R_a and R_b

represents the transcellular pathway, where R_a and R_b are the apical cell membrane and

basolateral cell membrane resistances, respectively. The sum of R_{tj} and R_{ic} represents the

paracellular pathway, where R_{ic} and R_{tj} are the intercellular resistances and the tight junction

resistances, respectively. R_a substances have a chance of travelling through the gap between the

transcellular and paracellular pathways instead of travelling through both pathways. R_{gap}

represents the partial coverage of the cell support, which includes only the membrane resistance

because the R_{gap} is developed as it is parallel to the transcellular and paracellular pathways. The simple circuit shown in **Figure 9** can be solved by taking the equivalent resistance of the resistors in transcellular and paracellular pathways, as two sets of resistors in parallel.

$$T_{TEER} = \frac{(R_a + R_b).(R_{ic} + R_{tj})}{(R_a + R_b) + (R_{ic} + R_{tj})} \qquad (1) \quad [1]$$

TEER measurements for the placenta-on-a-chip were calculated by two methods: theoretical and experimental. The next two sections describe both methods in detail. The purpose of having a theoretical method is to validate the results from experimental method.

5.3 Theoretical method

To build a theory for TEER measurements that explains the geometry and the behavior of the cell lines in channels, the placenta-on-a-chip is simplified with two parallel channels separated by a membrane. A simplified equivalent circuit is built by replacing resistors for the top channel, bottom channel, and membrane. In **Figure 10**, the top channel is represented by resistors R_a to R_d, including the resistance of the top channel above the membrane area, which is indicated as $R_{T1} \rightarrow R_{Tn-1}$. Similarly, resistance of the bottom channel is represented by the resistors R_c to R_b including the resistance of the bottom channel below the membrane, which is depicted as $R_{B1} \rightarrow R_{Bn-1}$. Resistance of the membrane, top channel above the membrane, and bottom channel below the membrane are calculated assuming the resistors on that specific area are distributed uniformly.

According to the above assumption, the calculation is simplified as $R_{T1} = R_{T2} = \cdots = R_{Tn-1}$ and $R_{B1} = R_{B2} = \cdots = R_{Bn-1}$ for top channel and bottom channel, respectively. The resistance of the channels above and below the membrane is equal to the reciprocal of the conductance of each channel over the length of the membrane [1]. **Equation 2** can be used to
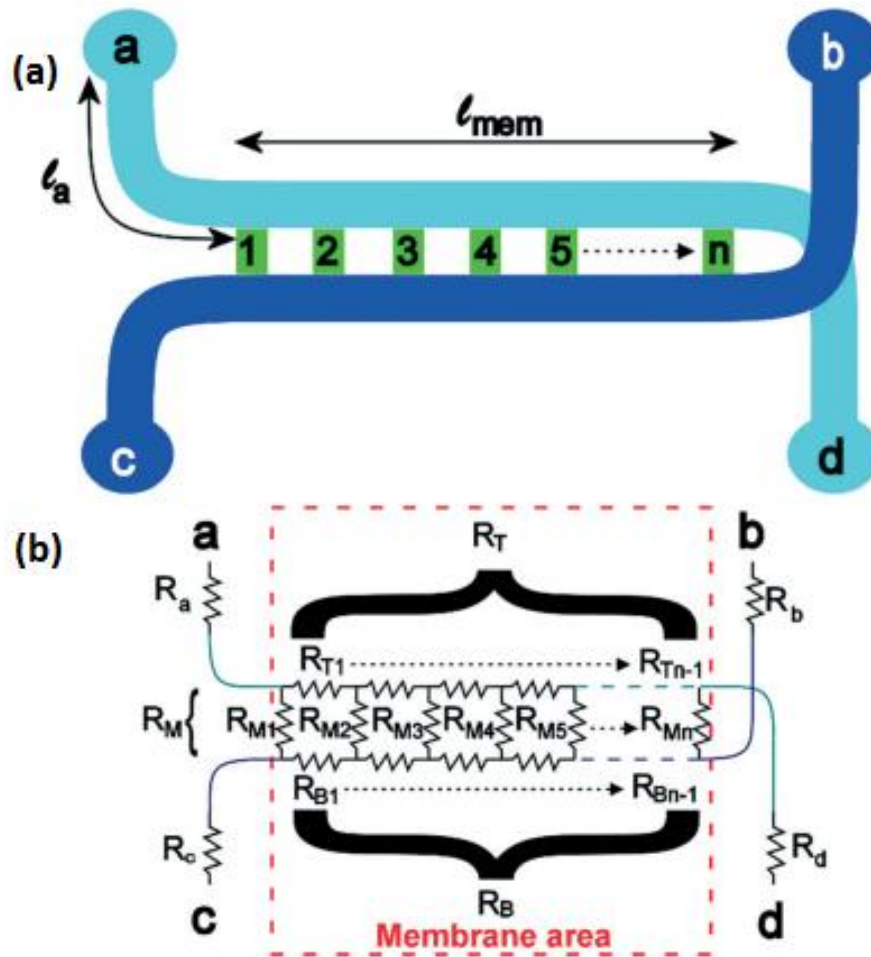

Figure 10: *Chip simplified to build the equivalent circuit, (a) layout of the chip, (b) circuit with resistors substituted for top channel, bottom channel and membrane. Reproduced from Odijk et al. [1] with permission of The Royal Society of Chemistry.*

calculate total resistance of each channel above and below the membrane. In **Equation 2**, l_{mem}, w_{ch}, and h_{ch} represent the length of the channel above/below the membrane, width of the channel, and height of the channel in meters, respectively. K is the conductivity of the cell medium (S m⁻

[1]) and n is the number of resistors on the area. Typically, 1000 resistors are ideal for the experiments to get more accurate results.

$$R_X = \frac{l_{mem}}{n.w_{ch}.h_{ch}.K} \qquad (2)^1$$

R_M to R_{Mn-1} resistors represent the membrane resistivity, which can be calculated using **Equation 3**. R_{TEER} is the TEER measurement taken under more ideal systems like with Transwell inserts, which can be found in literature. P is the porosity of the membrane (%) and h_{mem} is the thickness of the membrane. First and second terms represent the resistance due to cell support and resistance from the cell barrier, respectively.

$$R_{Mx} = \frac{h_{mem}}{P.w_{ch}.\frac{l_{mem}}{n}.K} + \frac{R_{TEER}}{w_{ch}.\frac{l_{mem}}{n}} \qquad (3)^1$$

Looking at the proposed circuit, theoretical resistance for R_{a-b} can be solved assuming n (number of resistors) approaches infinity. Following this, the two port system can be solved
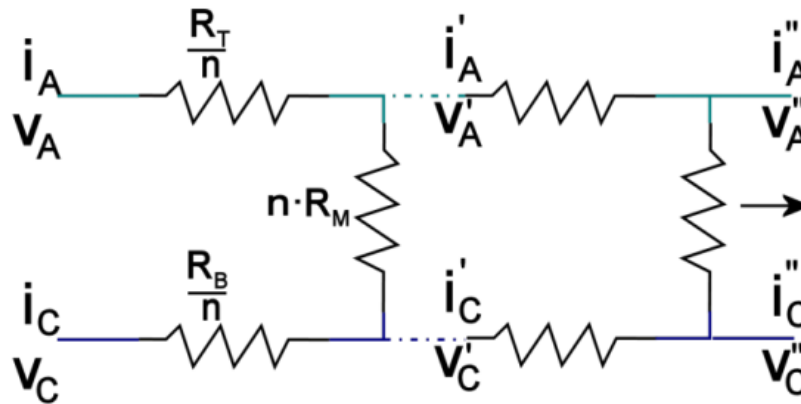

Figure 11: *Circuit simplified to show the ladder system, original figure was taken from supplementary materials of Odijk et al. Reproduced from Odijk et al.[1] with permission of The Royal Society of Chemistry.*

assuming the circuit consist of n section of simplified circuit denoted in V_A, V_A', V_C' and V_C in **Figure 11**.

Following solution is reproduced from Odijk et al.[1] with permission of The Royal Society of Chemistry.

Three new variables are introduced as R_m, R_t and R_b where,

$$R_m = R_M \cdot n \qquad (4)^1$$

$$R_t = \frac{R_T}{n} \qquad (5)^1$$

$$R_b = \frac{R_B}{n} \qquad (6)^1$$

The circuit shown in **Figure 11**, is a ladder network. By applying Kirchhoff's voltage law (KVL),

$$V_A' = V_A - R_t \cdot i_A \qquad (7)^1$$

$$V_C' = V_C - R_b \cdot i_C \qquad (8)^1$$

Applying Kirchhoff's current law (KCL),

$$i_A' = i_A - \frac{V_A' - V_C'}{R_m} \qquad (9.1)^1$$

$$i_C' = i_C + \frac{V_A' - V_C'}{R_m} \qquad (10.1)^1$$

Simplifying KCL equations using KVL equation,

$$i_A' = i_A - \frac{V_A - V_C - R_t \cdot i_A + R_b \cdot i_c}{R_m} \qquad (9.2)^1$$

$$i_C' = i_C + \frac{V_A - V_C - R_t \cdot i_A + R_b \cdot i_c}{R_m} \qquad (10.2)^1$$

For one section,
$$\begin{bmatrix} i_A' \\ i_C' \\ V_A' \\ V_C' \end{bmatrix} = \begin{bmatrix} 1 + {R_t}/{R_m} & -{R_b}/{R_m} & -1/{R_m} & 1/{R_m} \\ -{R_t}/{R_m} & 1 + {R_b}/{R_m} & 1/{R_m} & -1/{R_m} \\ -R_t & 0 & 1 & 0 \\ 0 & -R_b & 0 & 1 \end{bmatrix} \begin{bmatrix} i_A \\ i_C \\ V_A \\ V_C \end{bmatrix} \qquad (11)^1$$

For n sections and n→∞ (n = 1000 assumed to be large enough to get convergent results.)

$$
\begin{bmatrix} i_A{}^\infty \\ i_C{}^\infty \\ V_A{}^\infty \\ V_C{}^\infty \end{bmatrix} = \lim_{n\to\infty} \left[I + \begin{bmatrix} R_t/R_m & -R_b/R_m & -1/R_m & 1/R_m \\ -R_t/R_m & R_b/R_m & 1/R_m & -1/R_m \\ -R_t & 0 & 0 & 0 \\ 0 & -R_b & 0 & 0 \end{bmatrix} \right]^n \begin{bmatrix} i_A \\ i_C \\ V_A \\ V_C \end{bmatrix}
\qquad (12.1)^1
$$

$$
\begin{bmatrix} i_A{}^\infty \\ i_C{}^\infty \\ V_A{}^\infty \\ V_C{}^\infty \end{bmatrix} = \lim_{n\to\infty} \left[I + \frac{1}{n}\begin{bmatrix} R_T/nR_m & -R_B/nR_M & -1/R_M & 1/R_M \\ -R_T/nR_M & R_B/R_M & 1/R_M & -1/R_M \\ -R_T & 0 & 0 & 0 \\ 0 & -R_B & 0 & 0 \end{bmatrix} \right]^n \begin{bmatrix} i_A \\ i_C \\ V_A \\ V_C \end{bmatrix}
\qquad (12.2)
$$

Note that when n→∞,

$$
\lim_{n\to\infty} \left(\frac{R_T}{nR_M}\right)^n \to 0
$$

Similarly, when n→∞,

$$
\frac{-R_B}{nR_M}, \frac{-R_T}{nR_M}, \frac{R_B}{nR_M} \to 0
$$

Now compare the above equation with the well-known identity,

$$
e^A = \lim_{n\to\infty} \left(I + \frac{1}{n}A\right)^n
\qquad (13)
$$

Additionally,

$$
i_A{}^\infty = i_D, i_C{}^\infty = i_B, V_A{}^\infty = V_D \text{ and } V_C{}^\infty = V_B
$$

Using above values, results can be simplified to:

$$
\begin{bmatrix} i_D \\ i_B \\ V_D \\ V_B \end{bmatrix} = \exp\begin{bmatrix} 0 & 0 & -1/R_M & 1/R_M \\ 0 & 0 & 1/R_M & -1/R_M \\ -R_T & 0 & 0 & 0 \\ 0 & -R_B & 0 & 0 \end{bmatrix} \begin{bmatrix} i_A \\ i_C \\ V_A \\ V_C \end{bmatrix}
\qquad (14)^1
$$

Assume,

$$\exp\begin{bmatrix} 0 & 0 & -1/R_M & 1/R_M \\ 0 & 0 & 1/R_M & -1/R_M \\ -R_T & 0 & 0 & 0 \\ 0 & -R_B & 0 & 0 \\ & & 0 & 0 \end{bmatrix} = \begin{bmatrix} Z_{11} & Z_{12} & Z_{13} & Z_{14} \\ Z_{21} & Z_{22} & Z_{23} & Z_{24} \\ Z_{31} & Z_{32} & Z_{33} & Z_{34} \\ \mathbf{Z_{41}} & Z_{42} & Z_{43} & Z_{44} \end{bmatrix} \qquad (15)$$

This final equation is equivalent to hybrid parameter matrix model for a two port circuit. We are

interested in resistance between Ports A and B, assuming an input current i_A into port "A" (ie:

Term of our interest is V_B/i_A = resistance between Port A & B).

From the matrix equation above,

$$V_B/i_A = Z_{41} \qquad (16)$$

Note: In two port circuit theory, when two hybrid parameters are used:

$$Z_{41} = \frac{V_B}{i_A}\bigg|_{i_C = V_A = V_C = 0} \qquad (17)$$

By applying calculated values for $R_T, R_B \ and \ R_M$ from **Equation 2** and **Equation 3** to **Equation**

15, R_{a-b} can be solved. The theoretical TEER value can be calculated by multiplying the R_{a-b}

value by the membrane area $(w \times l)$.

5.4 Experimental method

   A simple TEER measuring instrument was built by connecting two 0.5mm x 0.6mm x

13mm Silver Chloride (Ag/AgCl) electrodes (DOCXS Biomedical) to a digital LCD multimeter

(Sinometer MS8261) by using regular multimeter probe cables, as shown in **Figure 12**. Then two

Ag/AgCl electrodes were connected to the end of two multimeter probe cables.

As shown in the **Figure 13**, one of the Ag/AgCl electrode was inserted into the inlet of the top channel, and other electrode was inserted into the outlet of the bottom channel. Then the resistance value was read from the multimeter. The resistance value read before growing any cells on channels by using the same inlet and outlet to use as the reference resistivity, which noted as R_{blank} in **Equation 16.**

$$R_{app,TEER} = (R_{cells} - R_{blank}).w_{ch}.l_{mem} \qquad (16)^1$$

Equation 16 was used to calculate the apparent TEER (the parameter most of the research papers used to report the TEER in oragn-on-chips devices), which used the measured resistance between two electrodes (R_{cells}) and subtracted the resistance value measured from the empty chip (R_{blank}), then multiplied the resultant value with the total membrane area ($w_{ch}.l_{mem}$).
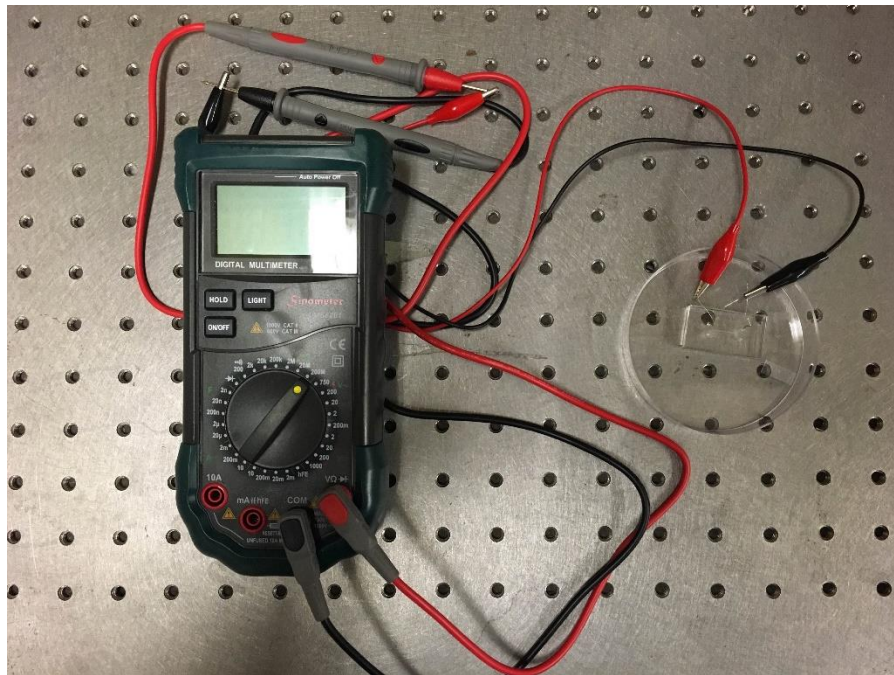

Figure 12: *Schematic of the experiment setup, Ag/AgCl electrodes connected to digital LCD multimeter (Sinometer MS8261) with probes. Original setup is used in Pemathilaka et al.[12]*
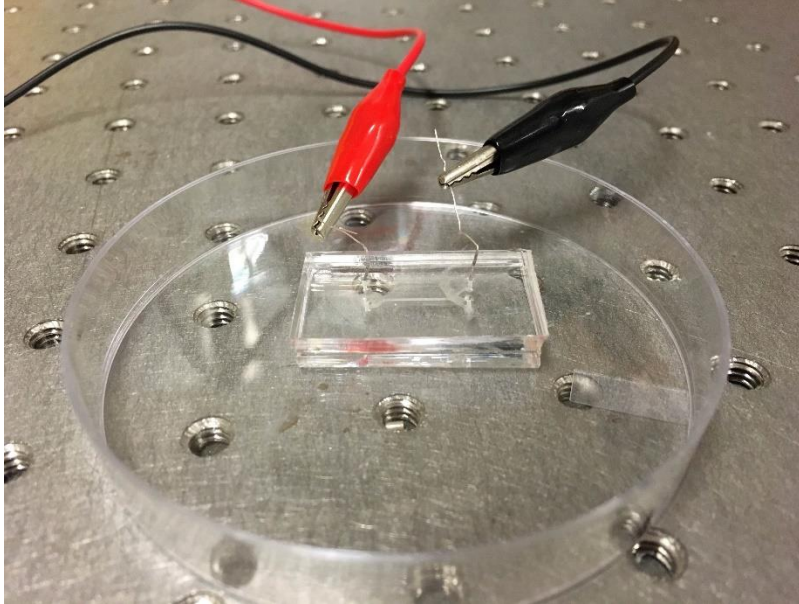
Figure 13: *Placenta-on-a-Chip with Ag/AgCl electrodes inserted to the inlet of the top channel and outlet of the bottom channel.*

5.5 References

1. Odijk, M., A. D. van der Meer, et al. (2015). "Measuring direct current trans-epithelial electrical resistance in organ-on-a-chip microsystems." Lab on a Chip 15(3): 745-752.

2. "Transcellular pathway." A Dictionary of Biology. 2004. Retrieved February 20, 2016 from Encyclopedia.com.

3. "Paracellular pathway." A Dictionary of Biology. 2004. Retrieved February 20, 2016 from Encyclopedia.com.

4. Abbott, N. J., L. Ronnback, et al. (2006). "Astrocyte-endothelial interactions at the blood-brain barrier." Nat Rev Neurosci **7**(1): 41-53.

5. Douville, N. J., Y.-C. Tung, et al. (2010). "Fabrication of Two-Layered Channel System with Embedded Electrodes to Measure Resistance Across Epithelial and Endothelial Barriers." Analytical Chemistry **82**(6): 2505-2511.

6. Cheung, K., S. Gawad, et al. (2005). "Impedance spectroscopy flow cytometry: On-chip label-free cell differentiation." Cytometry Part A **65A**(2): 124-132.

7. Pantoja, R., J. M. Nagarah, et al. (2004). "Silicon chip-based patch-clamp electrodes integrated with PDMS microfluidics." <u>Biosensors and Bioelectronics</u> **20**(3): 509-517.

8. Lagally, E. T.; Simpson, P. C.; Mathies, R. A. Sens. Actuators, B 2000, 63, 138–146.

9. Johnson, A. S., A. Selimovic, et al. (2011). "Integration of Microchip Electrophoresis with Electrochemical Detection Using an Epoxy-Based Molding Method to Embed Multiple Electrode Materials." <u>Electrophoresis</u> **32**(22): 3121-3128.

10. Morgan, H., M. P. Hughes, et al. (1999). "Separation of submicron bioparticles by dielectrophoresis." <u>Biophysical Journal</u> **77**(1): 516-525.

11. Sakmann, B., Neher, E., 1995. Single Channel Recording. Plenum, New York.

12. Rajeendra Pemathilaka, Jeremy Caplin, and Nastaran Hashemi, "Studying the Behavior in Organ-on-a-Chip with a Barrier Function of Epithelial and Endothelial Cell Monolayers" ASME 2015 4th Global Congress on NanoEngineering for Medicine and Biology, Minneapolis, MN, April 19-22, 2015.

CHAPTER 6

RESULTS AND DISCUSSION

Chapter 6 is focused on results and discussion for both placenta-on-a-chip model and TEER measurements.

6.1 Placenta-on-a-chip

As described in Chapter 4, HUVEC and BeWo cells were cultured until they reached to high density. Cells cultivated in low densities may result in low cell density inside the placenta-on-a-chip. **Figure 14** shows cultivated HUVEC and BeWo cells at a high density.
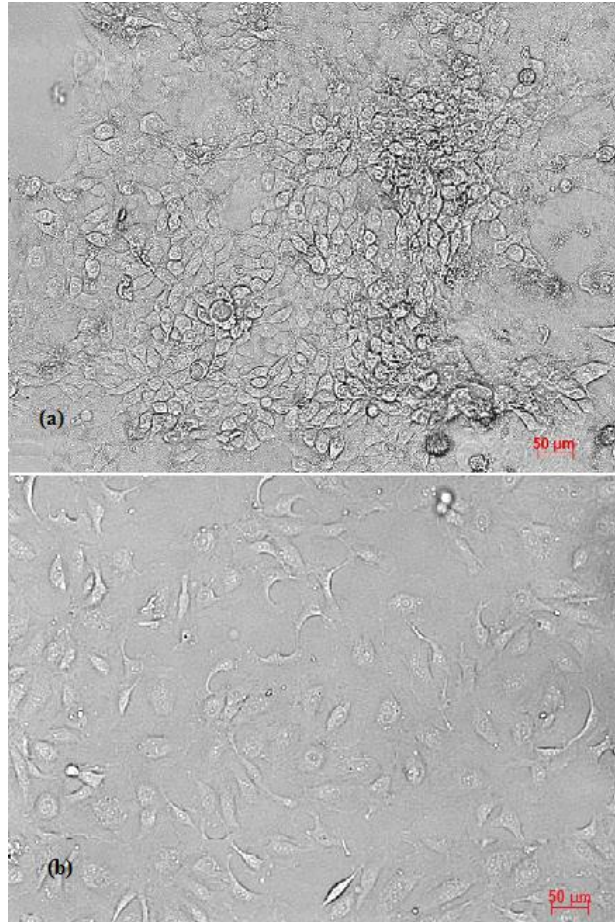

Figure 14: *Cell at high density, captured from ZEISS microscope,*
(a) BeWo cells, (b) HUVEC cells at 50 micron scale (10X).

During HUVEC cell culture, it was observed that HUVEC cells tend to attach to each other at higher densities. BeWo tended to grow into 3D structures at higher densities. This was observed in a different microscope. When performing the fluorescent imaging for HUVEC cells, we found that, in addition to staining the cells, the CellTracker stained other material on the surface of the flask. **Figure 15** shows the BeWo flask after fluorescent imaging.
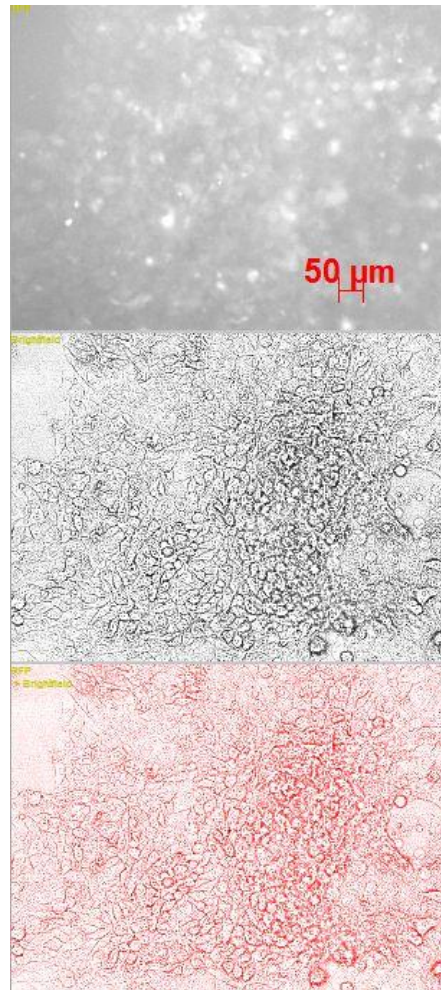

Figure 15: *A fluorescent image of BeWo cells after 45 minutes incubation with CellTracker^{TM} Orange CMRA fluorescent dye. The image was taken with a ZEISS microscope 10X.*

6.1.1 Cells inside the channels after adhesion period

As described in Chapter 4, green CMFDA fluorescent-stained HUVEC cells were injected to the top channel and incubated for 12 hours to help cell adhesion. **Figure 16** shows a fluorescent image of the chip after 12 hours.
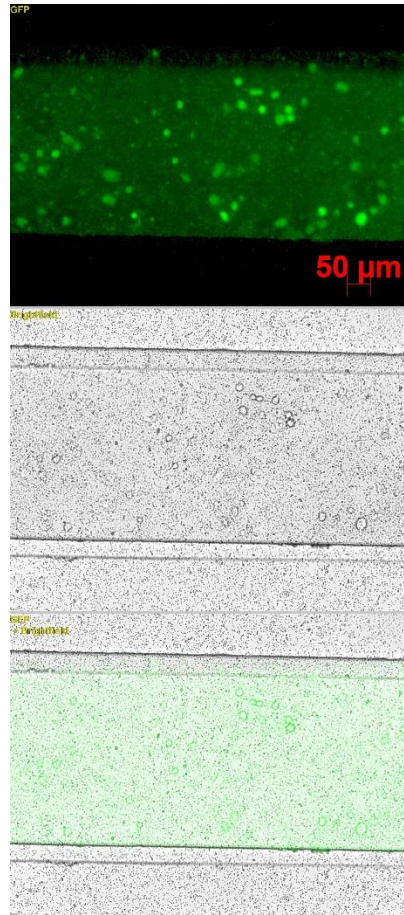

Figure 16: *HUVEC cells in the top channel of the placenta-on-a-chip after 12hrs of adhesion period, 10X-ZEISS microscope.*

A major problem with the HUVEC cells was, even when the suspended density was adjusted to 5×10^6 cells/mL, the membrane area of the top channel contained a low cell density. This was because most of the cells remained in space between the inlet side membrane end and inlet. To minimize this problem, cells were resuspended before taking them up with the

micropipette tip. However, this adjustment did not change the ultimate cell distribution. After the

12 hour period of the HUVEC cell adhesion, orange CMFDA fluorescent-stained BeWo cells

were injected into the bottom channel. Following the same procedures, top and bottom channels

were observed by fluorescent imaging. **Figure 17** shows a fluorescent image of the channels

with both HUVEC and BeWo cells after 12 hours of cell adhesion for BeWo, and 24 hours of
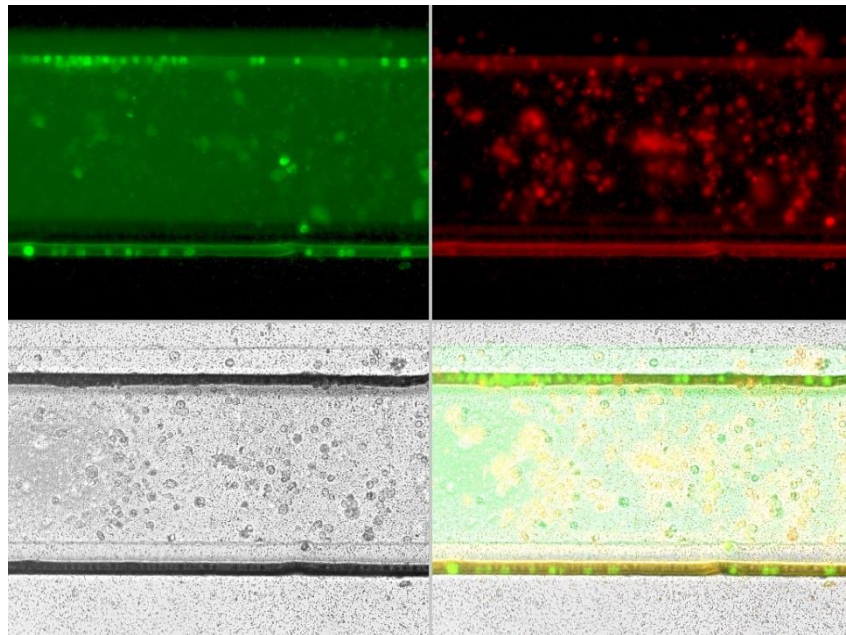
cell adhesion for HUVEC cells.

Figure 17: *Fluorescent image showing both HUVEC and BeWo cells*
inside the channels after 12 hours of BeWo adhesion. (t=24hours)

There is a clear indication from the GFP that most HUVEC cells are located toward the

edges of the channel. This may be due to two major reasons. First, while we kept the BeWo cells

on the chip for 12 hours, HUVEC cells were inside the chip for 24 hours. The second reason is

HUVEC cells did not attach to the membrane, so they were able to move freely. The main result,

if they did not attach to the membrane, is that those at the edges of the channel will be pushed

out from the outlet when perfusion started. Some of the unattached cells could be observed under

the microscope due to their motion.

6.1.2 Cells inside the channels during perfusion

After the adhesion period, medium perfusion was started. As described in Chapter 4, the

medium (EGM and F-12K) filled 3mL syringes were attached to a syringe pump. The syringe

pump was operated at different flow rates for various trials, but the minimum flow rate

(1µL/minute) the syringe pump could handle was chosen for the best results. Faster flow rates
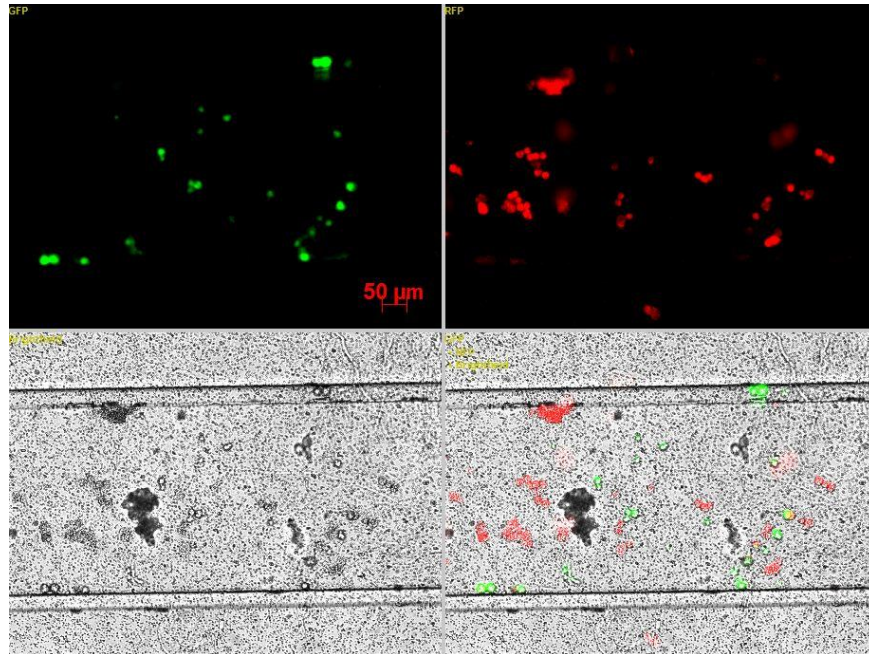

Figure 18: *Fluorescent image showing both HUVEC and BeWo cells inside
the channels after 24hours of medium perfusion. (t=48hours)*

could cause cells to peel off from the membrane while slower flow rates will not follow the

microfluidic flat form theory of representing an organ and also the same medium will be over the

cells for a long period. After 24 hours of medium perfusion, the chip was sent for fluorescent imaging.

As shown is **Figure 18**, fewer cells were identified in both channels than before perfusion. This may be due to the unattached cells observed before perfusion having been pushed out from the channels. Also, it was seen that a few air bubbles had developed inside the channels. Air bubbles build higher shear stresses on the surface, and this may be another main reason most of the cells (even the attached cells) were removed from the channels. The Microscopic brightfield image shows floating cells (middle dark spots). This was more visible under the
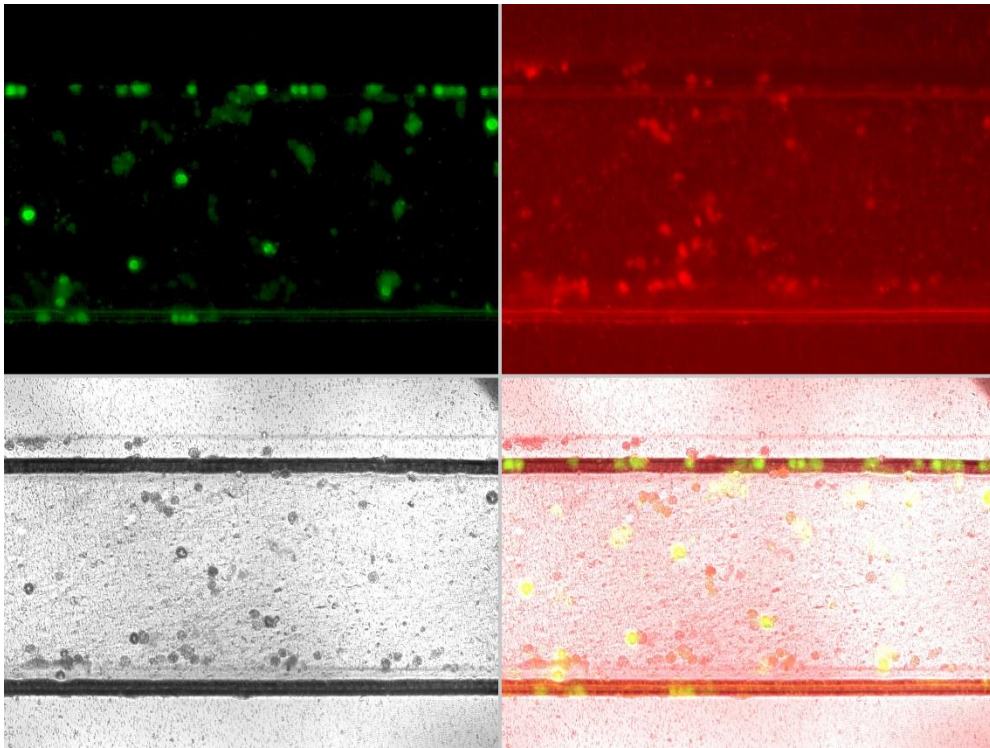

Figure 19: *Fluorescent image showing both HUVEC and BeWo cells inside the channels after 48hours of medium perfusion. (t=72hours), different position of the channel from Figure 5.*

microscope live image, rather than on the fluorescent image due to their motion.

After 48 hours of perfusion, the same position of the chip observed in **Figure 18** contained no cells (**Figure 19**). Most of the HUVEC cells had moved toward the edges of the channel. It was not confirmed if these cells were attached, but the apparent attachment could be due to imperfect alignment of the channels during manufacturing process, which could create a sharp edge on the channel that could prevent unattached cells from pushing off. In another position on the channel BeWo cells were found on the membrane area. Perfusion was continued for another 24 hours.
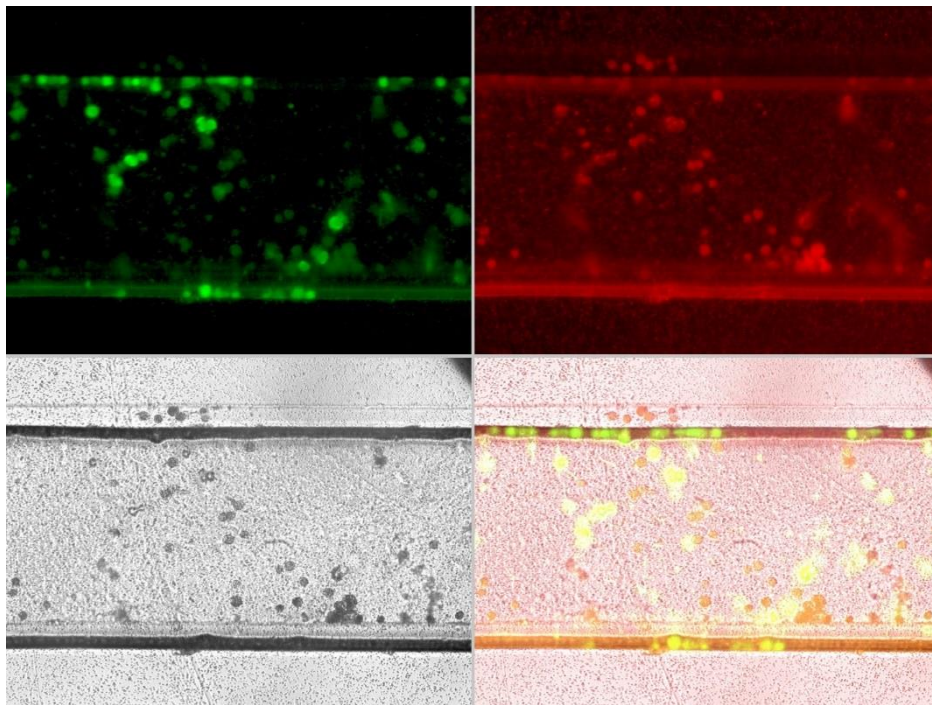

Figure 20: *Fluorescent image showing both HUVEC and BeWo cells inside the channels after 72hours of medium perfusion. (t=96hours).*

As shown in **Figure 20**, most of the HUVEC cells remained close to the edge. The GFP fluorescence showed lighter spots on the image that were not confirmed as cells. During the

perfusion, at least a small amount of medium could be transferred through the membrane. This small portion might be increased by the time. After 72 hours of medium perfusion (96 hours in total with the adhesion time), this medium might mix with the other channel's medium with the result of conflicting data. The perfusion was then continued for only 12 more hours.

After 84 hours of medium perfusion in total, the chip was again sent for fluorescent imaging. As shown in **Figure 21**, it became more difficult to identify the HUVEC cells on the top channel, but BeWo cells were somewhat visible in the bottom channel. A lack of cells and difficulty to take fluorescent imaging lead to stopping the perfusion after 84 hours of medium perfusion, 108 hours in total.
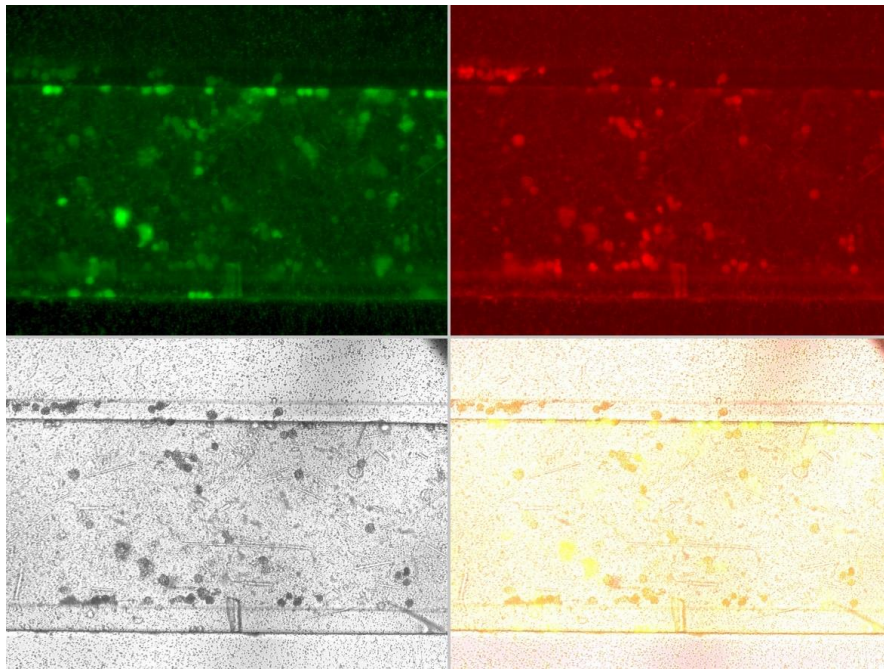

Figure 21: *Fluorescent image showing both HUVEC and BeWo cells inside the channels after 84 hours of medium perfusion. (t=108hours).*

6.2 TEER measurements

6.2.1 Experimental method

As described in Chapter 5, Ag/AgCl electrodes were inserted to the inlet of the top channel and the outlet of the bottom channel. The reason for using Ag/AgCl electrodes was because Ag/AgCl electrodes will measure the voltage while Ag electrodes will pass the current [1]. Resistance across two points was taken for empty chips and chips with cells on both sides of the membrane. Equation 6 (in Chapter 5) was used to calculate the Apparent TEER in Ohms-m^2. TEER values were taken every 12 hours or six hours depending on the trial. A graph was created using calculated Apparent TEER values (Ohms-m^2) vs. time (hours), as shown in **Figure 22**.
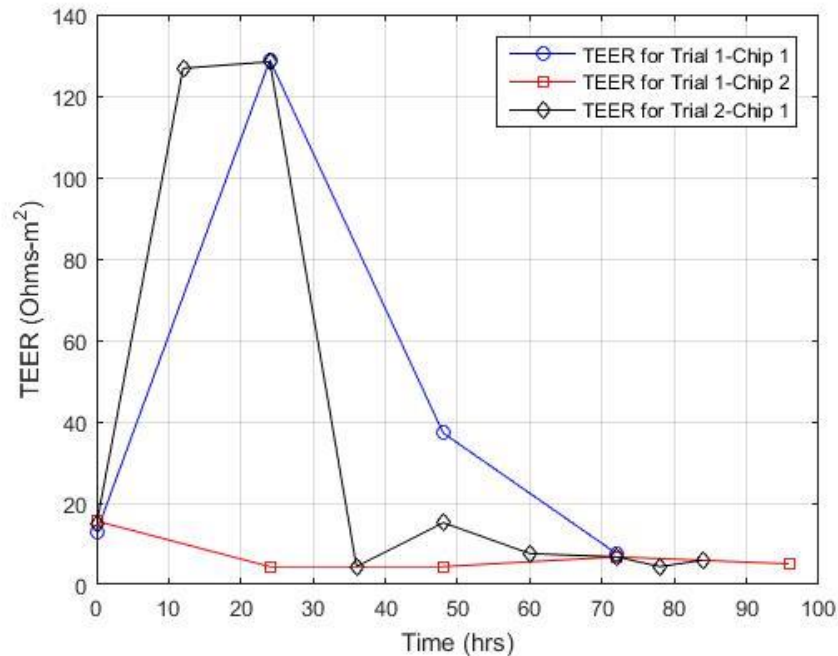

Figure 22: *Calculated Apparent TEER using resistance measured as described in Chapter 5, as a function of time. Three graphs represent three different trials as indicated in the legend.*

TEER values measured in an ideal system were expected to be increased by the time due to cell growth. Higher cell numbers would result in higher cell coverage across the cell culture surface (membrane in this experiment). With higher cell coverage, the number of tight junctions will increase. It was found that even a small percentage difference of cell coverage could cause about 80% lower TEER values compared to cell coverage at 100% [2]. This can be identified from **Figure 22**. Based on the discussion in Section 6.1.2, cell coverage was gradually decreased compared to the beginning of the experiment.

In Transwell systems, HUVEC cells remain in monolayers, but this is completely different in organ-on-chip devices. As Odijk et al.[2] explained from their experiment, after 72 hours of performance in their chip device, cells started to transform to a villi-like structure from the cells' original monolayer structure. This will limit the space in the channels and result in a higher value for top channel resistance. Another major issue that occurred during the TEER experiment was that fungus started growing in channels. As described earlier, this fungus could block the channel, resulting in an increase of the channel resistance.

Also, using Ag/AgCl electrodes could cause many other problems. When Ag/AgCl electrodes are inserted into the chip, they release silver ions.[3] The resistance then measured from the multimeter includes errors due to the toxicity of silver ions in the medium.[2] Resistance is also temperature dependent; TEER values calculated from values measured from the multimeter also contained errors due to a temperature effect.

6.2.2 Theoretical method

Using the theoretical model, two different TEER values were calculated. This was due to a system conflict with the experimental model. The theoretical model is designed to have only

one cell layer on one side while the other side is perfused with the same culture medium used for the cell layer. Two values were calculated as 48 Ωcm^2 and 111.4 Ωcm^2 by assuming HUVEC and BeWo cells were cultured on one side of the channel, respectively. The calculated values were much lower compared to TEER values obtained from Transwell cultures (HUVEC = 207Ωcm^2 and BeWo = 160 Ωcm^2).[4,5] As discussed earlier, TEER values measured in chip devices are different from TEER values obtained from Transwell cultures. The theoretical model needs to be modified to have two different cell types for this design. This can be simply done by separating the membrane resistance into two different sections. Assuming M_T and M_B are newly inserted parameters for the circuit, representing top membrane and bottom membranes, respectively, R_{M_T} and R_{M_B} can be separately calculated and the modified equation for R$_{MX}$ can be achieved.

6.3 References

1. CopyBook. (2016). Trans Epithelial Electric Resistance (TEER) Measurements. Retrieved February 20, 2016.

2. Odijk, M., A. D. van der Meer, et al. (2015). "Measuring direct current trans-epithelial electrical resistance in organ-on-a-chip microsystems." <u>Lab on a Chip</u> 15(3): 745-752.

3. Greulich, C., D. Braun, et al. (2012). "The toxic effect of silver ions and silver nanoparticles towards bacteria and human cells occurs in the same concentration range." <u>RSC Advances</u> **2**(17): 6981-6987.

4. Seok S.M., Kim J.M., Park T.Y., Baik E.J., Lee S.H., "Fructose-1, 6-bisphosphate ameliorates lipopolysaccharide-induced dysfunction of bloodbrain barrier." <u>Arch Pharm Res</u> 2013; 36: 1149–59.

5. Crowe, A. and J. A. Keelan (2012). "Development of a Model for Functional Studies of ABCG2 (Breast Cancer Resistance Protein) Efflux Employing a Standard BeWo Clone (B24)." <u>ASSAY and Drug Development Technologies</u> **10**(5): 476-484.

CHAPTER 7

CONCLUSION

7.1 Conclusion

In conclusion, the placenta-on-a-chip device was successfully designed for the engineering aspect of microfluidics. Chips were fabricated with PMMA milling and PDMS soft lithography techniques. PDMS chips were chosen for their ability to withstand lower thickness and for manufacturing simplicity. Cultured cells were injected onto the chips and successfully attached to the membrane. Cells were maintained long-term outside the incubator even with low cell densities inside the channels. Chips were able to be sent for fluorescent imaging without disassembling connecting tubes. It was discovered that, after 12 hours of cell adhesion, HUVEC cells were attached to the membrane, but after BeWo cells were injected and the chip kept for another 12 hours, most of the HUVEC cells were unattached. The 12 hour period of the cell adhesion period needs to be decreased. Alternatively, if BeWo cells take 12 hours to attach, perfusion for HUVEC cells should be started during the BeWo adhesion period. Also, it was discovered that imperfect alignment of channels during fabrication resulted in holding the cells close to walls, but this was mainly due to insufficient cell adhesion. Choosing a decent flow rate for the perfusion is important. Higher flow rates may result in forcing too much shear stress on the cells and lower flow rates may keep the same medium on cells for a longer time. Future work should be focused on increasing cell adhesion, perfecting channel alignment, and establishing suitable flow rates.

For TEER measurements, the proposed theoretical method was not able to provide accurate TEER values, as it was designed to represent one cell layer on one channel and medium

perfusion on the other channel. This method needs to be redesigned to represent current functions of the chip. Results with errors can be reduced, but some of the parameters are hard to control (i.e. the temperature effect). The only option to reduce the temperature effect is by accounting for errors due to temperature in the calculation. It was also discovered that removing connecting tubes and inserting Ag/AgCl electrodes to the inlet/outlet resulted in contamination. Two parallel experiments run with identical conditions, with and without measuring TEER, showed more contamination on the chip used for TEER measurements. The air bubbles that occurred inside the channels also resulted in errors, as the lack of medium in the channel may cause lower conductivity through the channel. Another problem discovered during the experimental method was that to study the TEER values as a function of time, required removing the connecting tubing, which caused the air bubbles occurring inside the channels that are difficult to remove. The only option was faster perfusion, which resulted in higher shear stress on cells, thereby forcing them to detach.

7.2 Future work

The following sections discuss some future work planned/needed to complete in the future.

7.2.1 Placenta-on-a-chip

For future work, various cell adhesion times can be considered. Changing the cell adhesion time may significantly affect the percent of cell confluency on the membrane. The flow rate is also a parameter to change, as higher and lower flow rates may result in cell detachment. Another concept for increasing the cell adhesion can be to make the membrane more adhesive.

This can be achieved by adding an extra ECM (extracellular matrix) layers such as fibronectin. After successfully culturing cell layers on both sides, the chip can tested in long-term maintenance. While in maintenance, various tests can be run on the system to verify the functionality of the chip to analyze similar physiological functions of placental barrier. A glucose test is a widely used method to analyze how the placental barrier functions. EBM-2 and F-12 mediums containing two different concentrations of glucose can be introduced to each channel. After some perfusion time, the output should be collected and a glucose monitoring test performed to see how well the barrier (membrane) functions similar to the real (*in vivo*) system. As a final goal, protein expression markers can be used to monitor transfer efficiency as well as to determine how similarly it represents the functions of the systems *in vivo*. Proteins such as Cadherin, type 1 transmembrane protein, provide more information on cell adhesion, as they are part of the adherence junction to bond cells in the tissues.

7.2.2   TEER measurements

As previous studies show, TEER is temperature dependent and the temperature effect needs to be accounted for in the measurements [1]. It is important to create a chip with confluent cell layers, because small errors in cell confluency can result in higher errors on TEER values. A more suitable way of inserting electrodes into the inlet/outlet of the chip needs to be found, as inserting electrodes frequently resulted in contamination. The theoretical method needs to be modified relevant to match the system with two cell types. TEER values for HUVEC cells and BeWo cells in Transwell cultures need to be verified, as the literature shows different values depending on different conditions and cell type.

References

1. Blume, L., Denker, M., Gieseler, F. and Kunze, T. Pharmazie, (2010). "Temperature corrected transepithelial electrical resistance (TEER) measurement to quantify rapid changes in paracellular permeability." <u>PubMed</u> 1, 19–24